https://doi.org/10.5194/egusphere-2026-1923
Preprint. Discussion started: 22 April 2026

Implications of glacier detachment triggered by a surge event at Dehdal Glacier in the Pamir Mountains, using daily PlanetScope imagery

Mustafo Safarov[1,2,3], Junli Li[1,3,*], Evan Miles[4,5,6,7], Majid Gulayozov[1,3], Ruonan Li[1,3,8], Ali Fazylov[9], Kamoliddin Nazirzoda[10], Firdavs Vosidov[1,11], Murodkhudzha Murodov[1,11], Hofiz Navruzshoev[11,12], Ardamehr Halimov[1,8,11]

[1]State Key Laboratory of Ecological Safety and Sustainable Development in Arid Lands, Xinjiang Institute of Ecology and Geography, Chinese Academy of Sciences, Urumqi 830011, China
[2]Research Center for Ecology and Environment of Central Asia (Dushanbe), Dushanbe 734063, Tajikistan
[3]Key Laboratory of GIS & RS Application Xinjiang Uygur Autonomous Region, Urumqi 830011, China
[4]Laboratory of Hydraulics, Hydrology and Glaciology (VAW), ETH Zurich, Zurich, Switzerland.
[5]Swiss Federal Institute for Forest, Snow and Landscape Research (WSL), bâtiment ALPOLE, Sion, Switzerland.
[6]Glaciology and Geomorphodynamics Group, Department of Geography, University of Zürich, Zürich, Switzerland.
[7]Department of Geosciences, University of Fribourg, Fribourg, Switzerland.
[8]University of Chinese Academy of Sciences, Beijing 100049, China
[9]Institute of Water Problems, Hydropower and Ecology of the National Academy of Sciences of Tajikistan, Dushanbe 734042, Tajikistan
[10]Center of glaciology Agency for hydrometeorology of the Committee for Environmental Protection under the Government of the Republic of Tajikistan, Dushanbe 734025, Tajikistan
[11]State Scientific Institution "Center for Research of Glaciers of the National Academy of Sciences of Tajikistan", Dushanbe 734025, Tajikistan
[12]Mountain Societies Research Institute, University of Central Asia, Dushanbe 734000, Tajikistan

Correspondence to: Junli Li (lijl@ms.xjb.ac.cn)

Abstract. Surge-type behavior and low-angle glacier detachments in small debris-covered mountain glaciers remain insufficiently documented. This study investigates the surge of the Dehdal Glacier in the northwestern Pamirs during 2025–2026, using daily PlanetScope satellite imagery. Multi-epoch uncrewed aerial vehicle (UAV) orthomosaics and digital elevation model (DEM) differencing from 2019 to 2023 reveal significant pre-surge internal mass redistribution, evidenced by surface thickening of the central tongue and surface lowering in both the upper glacier and the distal tongue, suggesting progressive internal destabilization. Demonstrated by PlanetScope imagery, the surge evolved through three distinct phases, which shows that surge initiation occurred internally and subsequently propagated down-glacier toward the terminus, resulting in detachments, accelerated ice flow, and reoccupation of the valley floor. Two low-angle detachments moved ice up to 4.7 km down-valley, depositing an estimated 4–5 × 10^6 m^3 of ice on the valley floor. By January 12, 2026, the glacier had largely stabilized, with the primary glacier tongue covering approximately 1.83 km^2 and a detached ice mass of about 0.26 km^2 persisting farther downstream, resulting in a total ice area of roughly 2.09 km^2. Notably, the recurrence interval of

https://doi.org/10.5194/egusphere-2026-1923
Preprint. Discussion started: 22 April 2026

9–10 years since the previous surge is significantly shorter than the earlier 20–30-year intervals. This shortened interval is unlikely to be due to seismic activity or to complete reservoir regeneration, and it occurred during warmer, drier conditions than the 1981–2010 baseline, which increased by +1.11 °C. These findings provide new insights into glacier flow instabilities in High Mountain Asia and highlight the geomorphic impacts of small glacier dynamics under increasing climatic stress.

1 Introduction

Surge-type glaciers represent a distinct class of dynamic ice masses characterized by quasi-cyclic transitions between prolonged quiescent phases and short-lived episodes of rapid flow (Meier and Post, 1969; Sevestre and Benn, 2015; Farinotti et al., 2020). During these surge phases, glacier velocities can increase by one to two orders of magnitude, leading to significant glacier advances, intense crevassing, and rapid redistribution of ice and debris onto valley floors (Raymond et al., 1987; Jiskoot, 2011). Such events can have a pronounced impact on downstream hydrology, temporarily block river channels, and trigger secondary geomorphic hazards (Muhammad et al., 2021; Murodov et al., 2024).

Despite decades of research, the coupled mechanical-hydrological processes governing the initiation, propagation, and termination of glacier surges remain incompletely understood (Kamb et al., 1985; Clarke, 1987; Fowler et al., 2001; Sevestre and Benn, 2015a; Benn et al., 2019; Lovell et al., 2026), especially in steep, debris-covered mountain glaciers, where factors such as basal drainage efficiency, enthalpy conditions, and valley confinement interact (Benn et al., 2012; Faillettaz et al., 2015; Gilbert et al., 2018). Various thermal, hydrological, and mechanical mechanisms have been proposed to account for surge behaviour, including transitions between cold-based and temperate basal regimes (Fowler et al., 2001; Sevestre et al., 2015b), pressurization of subglacial drainage systems, and stress redistribution within debris-covered tongues (Ravier et al., 2023; Sevestre and Benn, 2015a). However, most reconstructions rely on annual to multi-annual satellite observations (Quincey et al., 2011; Goerlich et al., 2020; Giullet et al., 2022), which are insufficient for capturing short-term kinematic transitions during surge onset, internally propagating stress fronts, or multi-phase detachment (Lovell et al., 2026).

Recent research in High Mountain Asia has identified instances of glacier detachment and large-scale ice failures in association with glacier surging (Leinss et al., 2021; Zou et al., 2023), but the transition from progressive surge acceleration to large-scale ice detachment remains poorly documented. These failures are characterised by rapid basal decoupling, structural failure, and significant mass displacement over low bed slope angles, representing an extreme case of dynamic instability. While these events share mechanical similarities with surge dynamics, such as basal decoupling and rapid mass displacement (Kääb et al., 2021), they are treated separately in the literature (Faillettaz et al., 2015; Zhang et al., 2023). The potential connection between classical surge behaviour and low-angle glacier detachment has not been thoroughly explored, especially in the context of small debris-covered glaciers in confined valleys (Leinss et al., 2021; Zhang et al., 2023).

The Pamir Mountains host one of the highest concentrations of surge-type glaciers globally (Osipova et al., 1998; Goerlich et al., 2020; Guillet et al., 2022; Guo et al., 2023). Historical and recent studies have documented numerous surge events and

https://doi.org/10.5194/egusphere-2026-1923
Preprint. Discussion started: 22 April 2026

their downstream impacts in this region (Lv et al., 2019; Wang et al., 2023; Safarov et al., 2024a). Many glaciers in the Pamirs are located in narrow, steep, debris-covered valleys, which enhance longitudinal stress transmission and strong glacier–valley coupling (Sevestre and Benn, 2015a; Guillet et al., 2022; Feroz et al., 2025). Studies documenting the full surge-detachment sequence at daily to weekly temporal resolution remain rare, limiting understanding of how internal glacier reorganization leads to downstream geomorphic impacts.

Recent regional inventories demonstrate that surge-type glaciers are widespread across High Mountain Asia (HMA) and exhibit strong spatial variability in surge style, timing, and geomorphic expression (Goerlich et al., 2020; Guillet et al., 2022; Beraud et al., 2025). However, there is limited direct observational evidence documenting the processes of surge initiation, propagation, detachment, and post-detachment adjustment at the daily scale, particularly for small debris-covered mountain glaciers. Although small mountain glaciers are usually thought to exhibit minimal dynamic variability, recent observations have revealed that even modest-sized debris-covered glaciers can undergo multi-phase surge or detachment behavior with considerable geomorphic implications (Rounce et al., 2020; Gilbert et al., 2018; Zou et al., 2023). Therefore, high-frequency documentation of complete surge-detachment sequences provides a valuable framework for examining surge mechanisms and their sensitivity to climate change.

The aims of this study are to: (1) quantify the rebuilding of Dehdal Glacier during the most recent quiescent period using multi-epoch UAV observations; (2) document the multi-stage surge sequence that occurred in 2025-2026, which includes two low-angle detachments; (3) evaluate potential climatic, geometric, and seismic factors that may influence this behaviour; (4) outline a research agenda for future investigations into similar surge-detachment-related hazards. To achieve these aims, we combined daily satellite imagery with multi-epoch UAV orthomosaics and DEM differencing to reconstruct the complete evolution of surge detachment on Dehdal Glacier.

2 Study Area

Dehdal Glacier (formerly Didal) (N38°59'20", E70°43'04") is located in the northwestern Pamir Mountains, Tajikistan, within the Surkhob River Basin, a major headwater tributary of the Vakhsh River that drains into the Amu Darya system (Fig. 1a–b). The glacier descends from the northern slopes of the Peter I Range (Peak Kaudal, 4775 m a.s.l.) and terminates in the upper Dara River valley (Safarov and Fazylov, 2023). The glacier covers approximately 1.6 km² in its quiescent state, and its tongue is confined within a narrow, steep valley, forming a debris-covered lower reach that directly interacts with the fluvial system and adjacent valley slopes (Fig. 1d). The Peter I Range is known for glacier detachments and rock-ice avalanche activity, and also hosts several surge-type glaciers (Leinss et al., 2021; Kääb et al, 2021).

Historical records indicate surge activity in 1897, 1974, 1995–1997, and 2015–2016 (Lipskiy, 1902; Kotlyakov et al., 2020). Earlier reports suggest a possible surge in either 1929 or 1939, although available evidence remains uncertain and aerial imagery from 1949 indicates the glacier was in a retreated state at that time. An analysis of mid-1990s Landsat TM imagery has revealed a previously unreported surge event between 1995 and 1997, characterized by a sudden down-glacier advance

https://doi.org/10.5194/egusphere-2026-1923
Preprint. Discussion started: 22 April 2026

and extensive crevassing. These records show a multi-decadal recurrence pattern, with surge intervals of approximately 20 to 35 years between the early-20th-century event and 1974, mid-1990s and the mid-2000s. During the surge from 2015 to 2016, the glacier advanced down-valley by about 1,950 m at an average rate of approximately 7.2 m d^{-1}, while the frontal position of the glacier remained stable and no significant breakaway occurred, unlike the one observed in 1974 (Rototayev, 1974; Kotlyakov et al., 2020; Desinov, 2021). In contrast, the surge sequence in 2025–2026 occurred only about 9 to 10 years after the 2015-2016 event. This represents the shortest documented recurrence interval for this glacier over the past century and involves renewed frontal reorganization, similar to the breakthrough described in 1974.

Additionally, unlike many surge-type glaciers in the Pamirs, the Dehdal Glacier is located near inhabited valleys and local infrastructure. This proximity increases downstream exposure to surge-related impacts, including rapid terminus advance, enhanced sediment delivery, short-term river-course reorganization, and associated natural hazards.

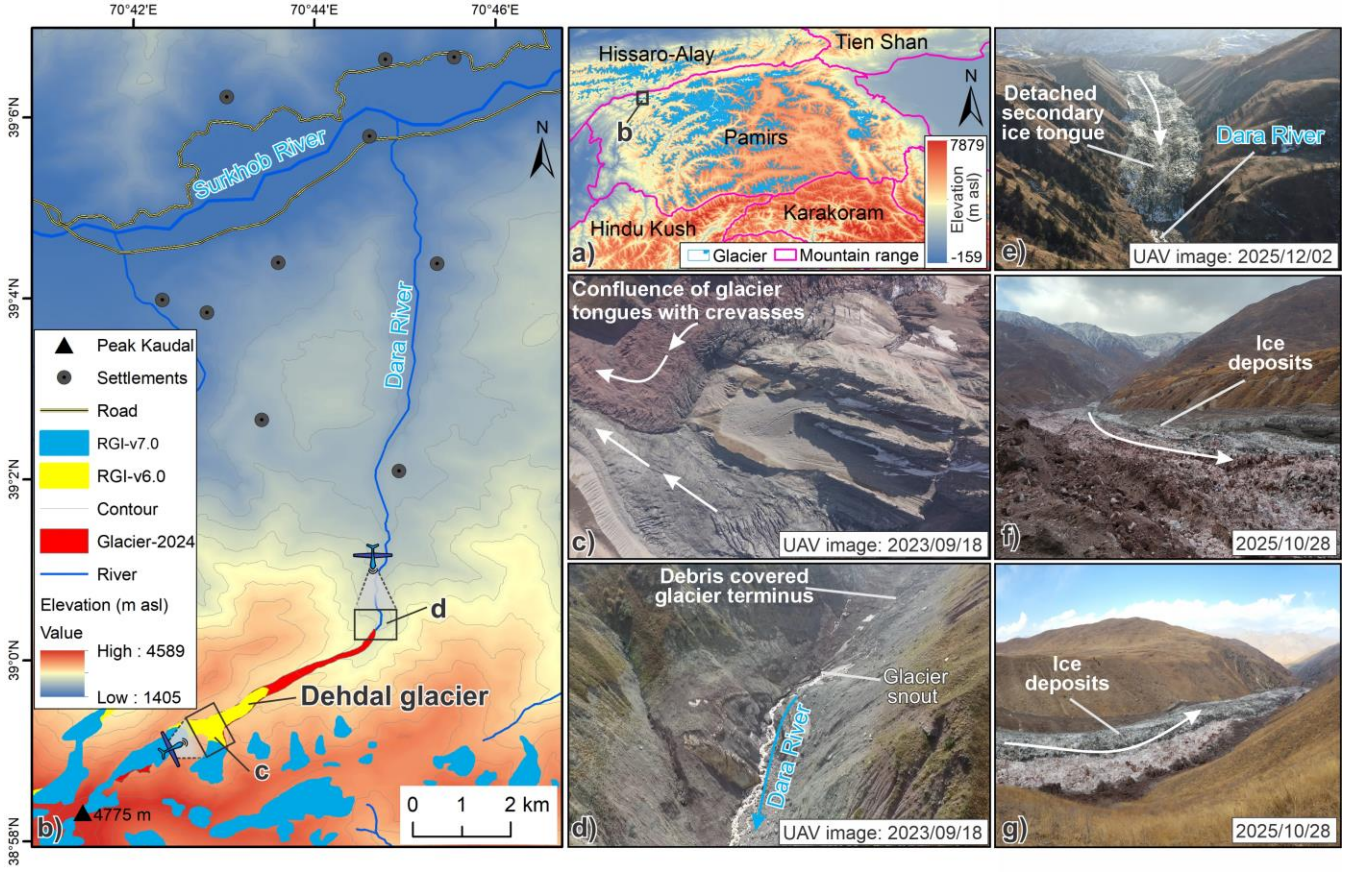

Figure 1: Location and geomorphological setting of Dehdal Glacier, northwestern Pamirs, Tajikistan. (a) Regional setting within High Mountain Asia. (b) Study area showing Dehdal Glacier and its drainage basin within the Dara and Surkhob river systems, with glacier outlines from the Randolph Glacier Inventory (RGI v6.0, v7.0) and updated 2024 outlines. (c) UAV orthomosaic showing crevasse and compressional structures in the upper glacier. (d) Debris-covered glacier terminus and its interaction with the Dara River. (e) Detached ice masses (secondary tongue) on the valley floor. (f–g) Debris-covered ice deposits and the down-valley extent of detached glacier material after the 2025 detachment events (photos: Kabutov).

https://doi.org/10.5194/egusphere-2026-1923
Preprint. Discussion started: 22 April 2026

3 Data and methods

3.1 Remote sensing datasets

PlanetScope satellite imagery has a spatial resolution of approximately 3 m, which has four-band Dove Classic/R products (blue, green, red, and near-infrared) before 2021 and eight-band surface-reflectance products (coastal blue, blue, green I, green, yellow, red, red edge, and near-infrared) after 2021 (Planet Labs PBC, 2026). We use PlanetScope satellite images to delineate glacier outlines, quantify terminus displacement, and track internal segmental motion along a central flowline, enabling reconstruction of surge onset, propagation, and late-phase evolution. To monitor glacier surging, dense time-series PlanetScope imagery was used to reconstruct the surging of the Dehdal Glacier between June 21 2025 and January 12 2026 (Table 1). A total of 128 cloud-free PlanetScope images were selected during the active surge phase to track frontal displacement and internal kinematic transitions, providing temporal resolution for quantitative analysis. Additionally, we selected September scenes from 2016 to 2024 to establish pre-surge reference conditions. Moreover, we also used Sentinel-2 Level-1C imagery (10 m spatial resolution) to complement PlanetScope observations during periods of incomplete coverage and to provide additional reference imagery for both pre-surge and surge conditions.

Table 1. Summary of remote sensing, field, and auxiliary datasets used to monitor Dehdal Glacier in the northwestern Pamirs, Tajikistan.

Dataset	Product / Platform	Spatial resolution	Temporal coverage	Usage / Purpose	Source
PlanetScope 8-band (SuperDove constellation) PlanetScope 4-band (Dove Classic/R)	PSScene (Surface Reflectance)	3 m	June 21 2025 – January 12 2026 (daily) Sep 2022–2024 (annual) Sep 2016–2021 (annual)	Primary dataset for mapping terminus displacement, surge evolution, and surface texture Pre-surge background glacier geometry	Planet Labs (Planet Explorer)
UAV orthomosaics & DSMs	QC-2 Micro UAV DJI Phantom 4	~15-30 cm	19 Jul 2019, August 11 2022, September 18 2023 August 8 2020, 23 Jul 2023, December 2 2025	High-resolution mapping of crevasses and surge morphology/ Visual observation of glacier terminus conditions	Field Survey
Sentinel-2 MSI	Level-1C	10 m	2025	Complementary glacier extent mapping and surface condition reference	Copernicus Data Space Ecosystem
AW3D30	ALOS PRISM (optical stereo)	30 m	~2006–2011	Regional topographic context	Japan Aerospace Exploration Agency (JAXA) / OpenTopography
ERA5-Land reanalysis	ECMWF	0.1°	2019 – 2025 (monthly)	Air temperature and precipitation context	European Centre for Medium-Range Weather Forecasts & Google Earth Engine
RGI glacier outlines	RGI v6.0 & v7.0	–	v6.0 (~2000); v7.0 (~2018)	Baseline glacier extents for comparison	Randolph Glacier Inventory
Regional seismicity	USGS Earthquake Catalog	–	2019–2025	Contextual assessment of seismic activity	USGS Earthquake Hazards Program

https://doi.org/10.5194/egusphere-2026-1923
Preprint. Discussion started: 22 April 2026

To document the fine-scale surface structures and terminus morphology following the second detachment event, a high-resolution image from the Luojia-1A satellite, provided by Wuhan University, was utilized. This image was captured on November 9, 2025, and has a spatial resolution of 0.5 meters. Additionally, digital elevation data from the AW3D30 global digital elevation model (30 m spatial resolution), derived from ALOS PRISM stereo imagery and accessed via OpenTopography, was used to provide topographic context and support analysis of glacier geometry and valley morphology. The slope of the lower glacier tongue was estimated from a Google Earth Pro elevation profile extracted along the central flowline of the lowermost ~1 km of the glacier tongue, yielding a mean slope of ~13°, with local slopes reaching ~28°.

Multi-epoch UAV surveys conducted on July 19 2019, August 11 2022, and September 18 2023 were used to generate centimetre-scale orthomosaics and digital elevation models (DEMs) (Fig. S1) to characterise the geomorphological structure of the glacier tongue and the upper confluence zone (Mishra et al., 2023). These UAV-derived products reveal crevasses, compressional ridges, and debris-covered ice morphology and serve as key reference information for interpreting pre-surge surface deformation patterns. Additionally, field-based visual observations of the glacier terminus were conducted on August 8 2020, July 23 2023, and December 2 2025 to provide qualitative ground reference for terminus position and post-surge surface conditions. The volume of the detached ice deposit estimated using cross-sectional thickness measurements derived from the UAV-based three-dimensional terrain model acquired on December 2 2025. Cross-valley profiles oriented approximately perpendicular to the valley axis were extracted to estimate local deposit thickness from the elevation difference between the pre-event valley surface and the post-detachment ice surface. Mean thickness derived from multiple cross-valley profiles combined with the mapped deposit area to obtain a first-order estimate of detached ice volume.

3.2 Surface velocity estimation

Surface velocity fields were derived from PlanetScope satellite imagery using feature-tracking via normalized cross-correlation (NCC) implemented in a custom MATLAB workflow. Image pairs were selected for late ablation-season conditions (September–September intervals) to minimize seasonal variability and ensure consistent interannual comparisons. Before estimating displacements, the image pairs were co-registered using a translation-based image registration method to reduce geometric offsets between scenes. Surface displacements were calculated by applying NCC template matching within predefined search windows to track stable surface features, which is a well-established method for estimating glacier motion from optical satellite imagery (Scambos et al., 1992; Kääb, 2005; Heid and Kääb, 2012; Dehecq et al., 2015). Displacement vectors were transformed into surface velocities using the time interval between image pairs, and low-correlation matches were filtered out before interpolating the velocity field to full image resolution.

For each grid node, a template window of 96 × 96 pixels (approximately 288 × 288 m) from the reference image was matched within a search window of 384 × 384 pixels (about 1152 × 1152 m) in the target image. These window sizes were selected to balance spatial resolution and displacement detectability while maintaining stable correlations over debris-covered glacier surfaces, following commonly applied optical feature-tracking approaches. Displacements were calculated on a regular grid with a step size of 48 pixels (about 144 m). Windows with insufficient surface texture were excluded using

https://doi.org/10.5194/egusphere-2026-1923
Preprint. Discussion started: 22 April 2026

a minimum standard deviation threshold of 0.01, and windows containing more than 20% missing data were discarded. The location of the NCC peak provided horizontal offsets (dx, dy) in pixel units. The offsets were converted to metres using the PlanetScope pixel size of 3 m. Velocities were calculated by dividing the displacement by the acquisition interval and expressed in m yr^{-1} for annual comparisons. Velocity uncertainty was estimated using apparent displacements measured over stable off-glacier terrain. Because the image resolution and feature-tracking parameters were consistent for all image pairs, a representative uncertainty estimate derived from stable terrain was assumed to apply to all velocity fields.

Velocity fields were generated for eight consecutive annual intervals, spanning from 2016–2017 to 2023–2024. A fixed visualization range of 0–800 m yr^{-1} was applied to all maps to facilitate direct interannual comparison. To represent the interannual background state for the period from September 24, 2024, to August 20, 2025, a long-term baseline of ~330 days was used to obtain spatially averaged annualized values, expressed in meters per year (m yr^{-1}), representing the pre-surge reference regime. Short-term surge dynamics were examined using sequential PlanetScope image pairs spanning 8–32 days during August to December 2025. For these short-term intervals, displacement vectors were converted to velocities expressed in m d^{-1}. Low-confidence matches were eliminated using a correlation threshold of Cmax < 0.50, ensuring that only displacement vectors with robust correlation scores were retained. To ensure comparability across event periods, a fixed velocity range of 0–60 m d^{-1} was applied to all short-term maps. Low-correlation pixels and shadow-affected regions were masked prior to analysis. Winter scenes with extensive fresh snow cover were excluded due to reduced feature-tracking reliability.

Two central flowlines were digitized following the principal glacier flow paths. Flowline A follows the right tributary branch and continues along the downstream trunk, whereas Flowline B traces the left tributary of the glacier. Surface velocities were sampled at regular intervals along each flowline to construct longitudinal velocity profiles for the 2016–2024 interannual period and for the 2025-2026 surge phase. This approach enables the identification of branch-scale asymmetry, spatial localization of acceleration, and multi-year patterns of glacier flow evolution.

3.3 Climatic and auxiliary data

Near-surface air temperature and precipitation were derived from the ERA5-Land reanalysis (ECMWF) using Google Earth Engine (GEE). We used the ERA5-Land Monthly Aggregated product (ECMWF/ERA5_LAND/MONTHLY_AGGR) at 0.1° × 0.1° spatial resolution (Hersbach et al., 2020). Monthly values were extracted for the grid cell containing Dehdal Glacier and analysed for the period 2016–2025 to characterise climate variability during the most recent decade. For baseline comparison, we computed the monthly climatology for 1981–2010 and expressed anomalies for 2016–2025 as differences relative to this baseline.

ERA5-Land monthly series were compared with observations from the Tojikobod meteorological station (39.1148° N, 70.8366° E; 1589 m a.s.l.; ~15 km from the glacier), operated by the Agency for Hydrometeorology of Tajikistan, for the period with overlapping records (available from 2020 onward). This comparison was used as a consistency check of the

https://doi.org/10.5194/egusphere-2026-1923
Preprint. Discussion started: 22 April 2026

reanalysis background climate signal, while recognising elevation and representativeness differences between the low-elevation station and the glacier environment.

Regional seismicity was assessed using the USGS Earthquake Catalogue. All earthquakes with magnitudes ≥ 3.5 within 60 km of Dehdal Glacier during 2019–2025 were extracted to evaluate possible temporal coincidence with surge initiation. Historical glacier outlines were obtained from the Randolph Glacier Inventory (RGI v6.0 and v7.0) provided by the National Snow and Ice Data Center (RGI Consortium 2017; RGI Consortium 2023) and used as standardized baseline references to compare long-term glacier geometry with PlanetScope-derived outlines.

3.4 Flowline definition and surge quantification

A central flowline representing the principal ice-flow axis of Dehdal Glacier was manually digitized using PlanetScope imagery acquired during the 2025-2026 event. All distances were referenced to the terminus position on August 20 2025, which served as the baseline zero point. Terminus displacement was quantified by projecting successive terminus positions onto the central flowline and measuring cumulative downstream distance relative to the zero point. This produced a continuous time series of longitudinal displacement, enabling identification of surge onset, acceleration phases, and termination.

In addition to terminus advance, segmental ice displacements occurring within the glacier tongue were mapped by tracking the longitudinal position of crevasse-bounded ice slabs migrating along the same flowline. Negative displacement values indicate up-glacier segmental motion.

3.5 Uncertainty assessment

Surface velocity uncertainty was assessed empirically using apparent velocities measured over stable off-glacier terrain. Three manually delineated stable reference polygons on bedrock slopes adjacent to the glacier were used to extract velocity data outside the glacier area. The residual bias was quantified using the median apparent velocity, while measurement uncertainty was estimated with the normalized median absolute deviation (NMAD).Horizontal displacement uncertainty is controlled primarily by PlanetScope geolocation accuracy and manual delineation uncertainty and was estimated as a nominal spatial uncertainty equivalent to approximately ±1 pixel (3m), following Paul et al. (2017) and Tarca et al. (2023). Temporal uncertainty is controlled by image acquisition frequency. During the 2025-2026 surge, observation intervals ranged from 1–7 days, constraining surge phase transitions within ±3 days.

Photogrammetric processing of UAV images was performed in Pix4Dmapper using standard structure-from-motion workflows, with manual tie points (MTPs) introduced during the bundle adjustment stage (Safarov et al., 2024b). DEM co-registration between UAV resurveys was evaluated using established off-glacier stability approaches outlined by Immerzeel et al. (2014), Xue et al. (2021), and Safarov et al. (2024b). Several stable, non-glaciated reference zones were delineated around the glacier tongue (Fig. S2). Elevation differences were extracted within these zones and used to quantify co-registration accuracy (Immerzeel et al., 2014; Lamsters et al., 2022). Additional uncertainty arises from UAV positioning

https://doi.org/10.5194/egusphere-2026-1923
Preprint. Discussion started: 22 April 2026

accuracy, GPS measurement limitations, lens distortion effects, flight altitude variability, and illumination differences between surveys (Wheaton et al., 2010; Clapuyt et al., 2017). These factors may introduce local geometric distortions and affect the precision of derived elevation products.

4 Results

4.1 Pre-surge geometry and baseline conditions

PlanetScope imagery indicates that Dehdal Glacier remained comparatively stable during 2016–2024, with no evidence of terminus advance. This pre-surge configuration provides the baseline against which the abrupt dynamic reorganisation in 2025 is distinguished. In August 2025, the lower tongue exhibited spatially heterogeneous frontal behaviour, with adjacent sectors showing localised advance and retreat, contrasting with the more uniform post-surge geometry observed in 2016 (Fig. 2). The satellite images highlight two zones of distinct surface morphology in August 2025, including the development of darkened zones of dense crevasse openings in the advancing upper sector, in contrast to a homogeneous and smooth surface appearance in the retreating lower sector.

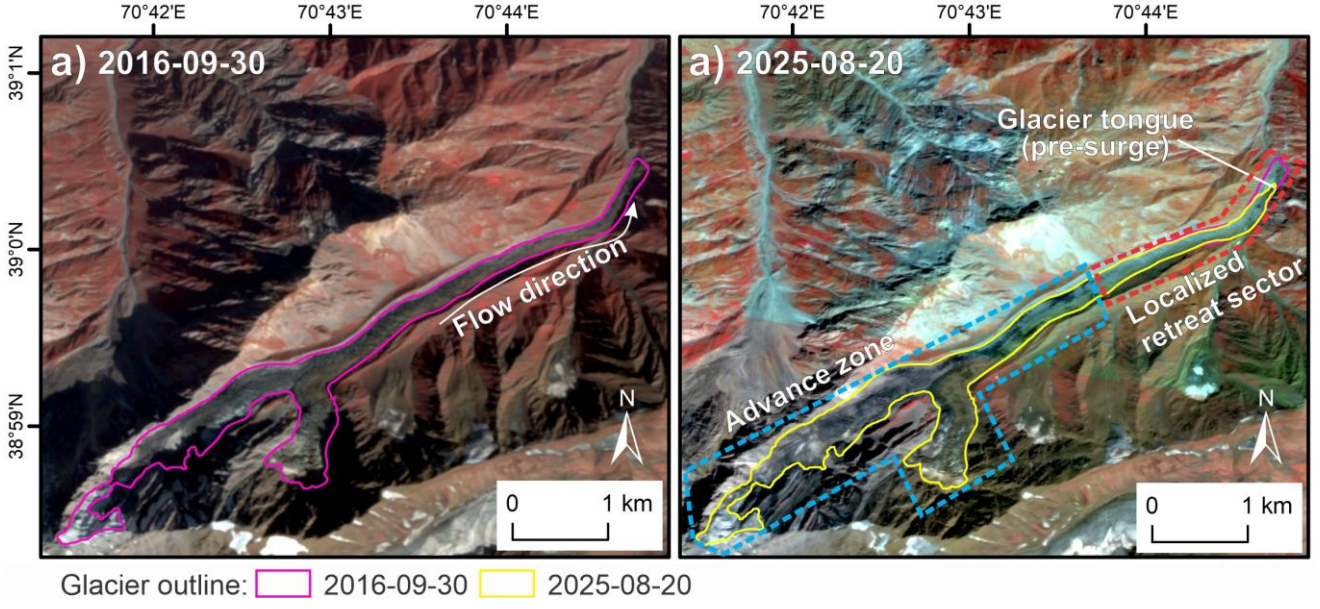

Figure 2: Glacier tongue configuration after the 2016 surge (September 30, 2016) and before the 2025-2026 surge (August 20, 2025). Solid outlines indicate glacier margins at the respective dates. Dashed polygons mark advance and localised retreat sectors observed in August 2025. Arrows denote the general ice-flow direction.

High-resolution UAV surveys conducted from 2019 to 2023, prior to the 2025–2026 surge, reveal that the glacier's lower tongue is heavily debris-covered, and a feature typical of quiescent surge-type glaciers in the region. This tongue features complex surface structures, including crevasses and compressional ridges (Fig. 1c–d), indicating a dynamically active and structurally complex tongue before the 2025 event. Importantly, the UAV-derived DEMs reveal pronounced surface-

https://doi.org/10.5194/egusphere-2026-1923
Preprint. Discussion started: 22 April 2026

elevation changes in the years preceding the 2025-2026 surge, with distinct spatial patterns of thickening and thinning. DEM differencing for the periods 2019–2022, 2022–2023, and 2019–2023 shows marked and persistent surface thickening in the central part of the glacier, reaching several tens of metres locally (Fig. 3a–c). This build-up is particularly evident along the debris-covered tongue and adjacent lateral moraines, consistent with ice-mass accumulation visible in the UAV orthomosaics and contemporaneous PlanetScope imagery.

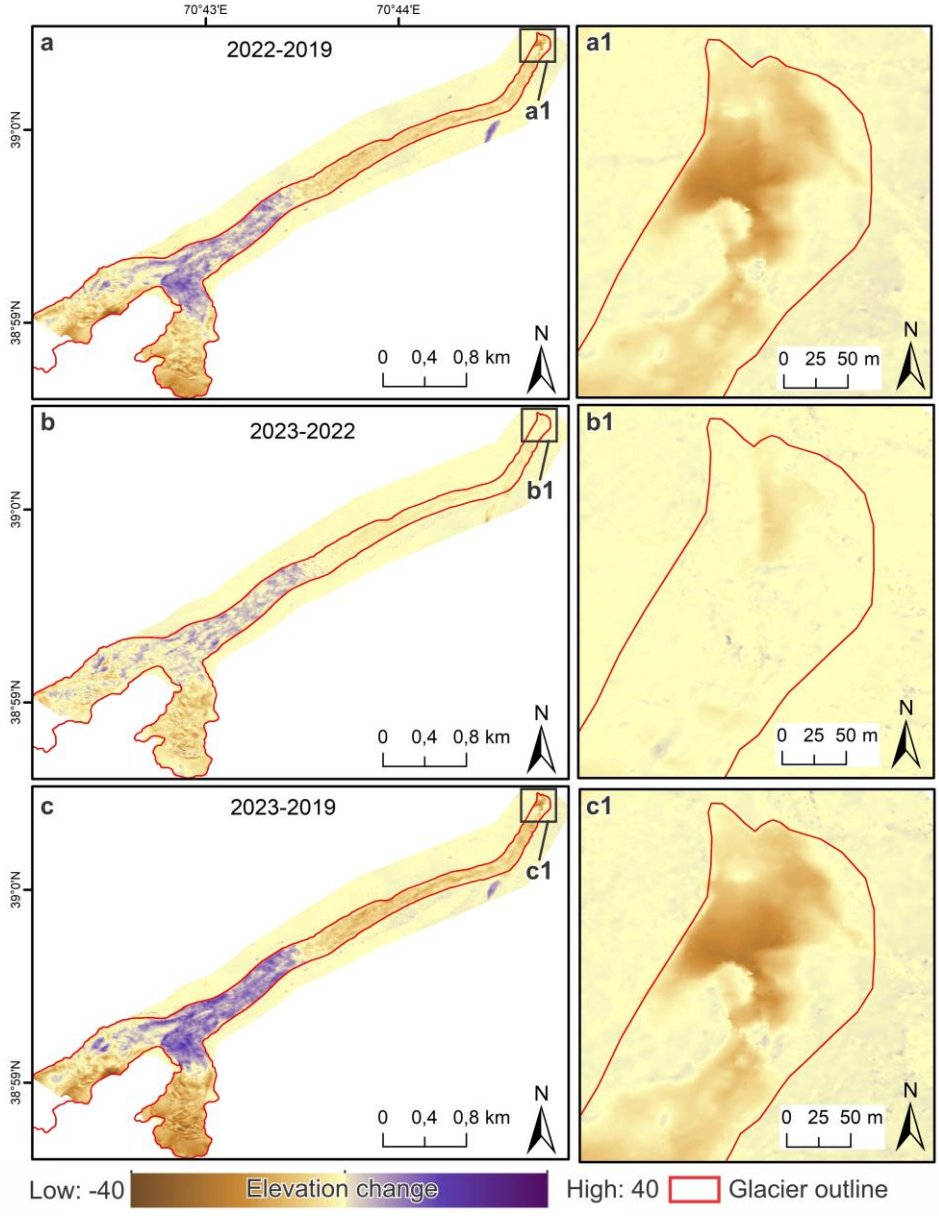

Figure 3: Glacier surface elevation changes derived from UAV DEM differencing for the periods 2019–2022 (a), 2022–2023 (b), and 2019–2023 (c). Panels (a1–c1) show zoomed views of the lower tongue. Positive values indicate surface thickening (m), while negative values indicate surface lowering (m).

https://doi.org/10.5194/egusphere-2026-1923
Preprint. Discussion started: 22 April 2026

At the same time, the lowermost downstream tongue exhibits net surface lowering over the same intervals (Fig. 3a1–c1), indicating progressive thinning and retreat in the distal part of the glacier. Central thickening combined with thinning in both the upper glacier and the distal tongue indicates strong spatial variability in surface-elevation change, reflecting the redistribution of ice within the glacier prior to the 2025-2026 surge. This pattern is consistent with reservoir-receiving zone mass transfer commonly observed prior to surge activation in surge-type glaciers (e.g., Sevestre and Benn, 2015; Goerlich et al., 2020; Murodov et al., 2024).

The sustained central thickening combined with downstream thinning raises the question of whether this represents a typical surge build-up stage. The UAV data indicate that, despite the relatively short quiescent period since the 2015–2016 surge, Dehdal Glacier underwent pronounced internal reorganisation prior to 2025. The magnitude and localisation of thickening emphasize the glacier's inability to efficiently evacuate mass from the central part of the glacier tongue, preconditioning the glacier for surge initiation. The driver of this discontinuity in ice flux, in terms of process and location, is a key unknown. Nevertheless, this pre-surge behaviour provides critical insight into the glacier's subsequent dynamics. It underscores the value of high-resolution elevation data for resolving surge-preparation processes in small, debris-covered mountain glaciers. The mean vertical elevation difference within off-glacier reference areas was ±0.5 m, while the mean horizontal offset was ±0.6 m, indicating good geometric consistency between UAV resurveys.

Surface velocities remained low and spatially uniform between 2016 and 2018, with maximum values generally below ~50 m yr^{-1} along both flowlines (Fig. 4). A first localized acceleration developed in 2018–2019, with velocities exceeding 400 m yr^{-1} in the lower portion of the upper basin. This episode was spatially confined and did not propagate throughout the glacier trunk. In 2019–2020, the glacier exhibited a sharp and localized velocity maximum of ~600 m yr^{-1} centered near 4.0–4.3 km. However, this acceleration was transient and followed by partial deceleration in 2021–2022. From 2022 onward, renewed and more spatially extensive acceleration developed along Flowline A. In 2023–2024, velocities exceeded 400 m yr^{-1} and were concentrated between approximately 4.5 and 5.2 km along the right tributary. The persistence of this spatially localized velocity core across multiple years indicates progressive mechanical preconditioning rather than abrupt surge initiation. These results demonstrate that the 2025-2026 surge-detachment sequence was preceded by multi-year dynamic reorganization localized within the right tributary.

Velocity uncertainty was evaluated using apparent velocities measured over stable off-glacier terrain. The stable-terrain analysis reveals a residual bias of 3.17 m yr^{-1} and an NMAD uncertainty of 0.28 m yr^{-1} for the annual velocity data. For the short-term velocity fields, the median apparent velocity over stable terrain is 0.17 m d^{-1}, with an NMAD of 0.13 m d^{-1}. These uncertainty values are significantly smaller than the glacier velocities observed during the surge phase.

https://doi.org/10.5194/egusphere-2026-1923
Preprint. Discussion started: 22 April 2026

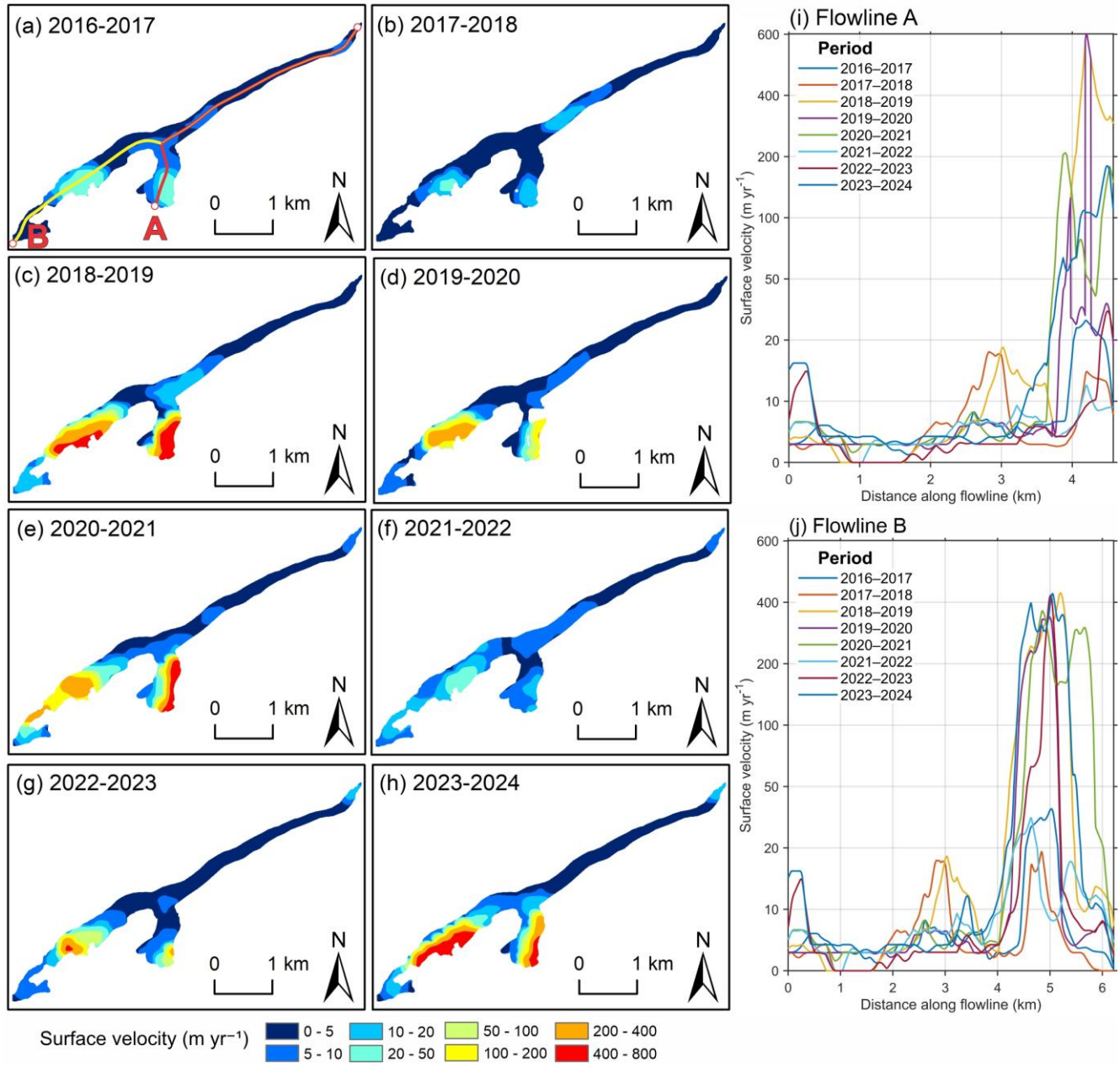

Figure 4: Interannual surface velocity evolution and longitudinal flowline profiles (2016–2024). (a–h) Annual September-to-September surface velocity fields based on PlanetScope satellite imagery. Velocities are shown on a fixed scale (0–800 m yr⁻¹) to allow direct interannual comparison. Flowlines A (right tributary and trunk) and B (left tributary) are indicated in panel (a). (i) Longitudinal velocity profiles along Flowline A. (j) Longitudinal velocity profiles along Flowline B.

4.2 Surge evolution and step-like frontal displacement

The 2025-2026 surge of Dehdal Glacier exhibited a multi-phase evolution punctuated by two low-angle detachment events, each leading to discrete frontal displacements, rather than continuous advance (Figs. 5-7). From June 21 to September 17,

https://doi.org/10.5194/egusphere-2026-1923
Preprint. Discussion started: 22 April 2026

2025, the glacier front remained confined. It did not extend beyond the defined 0-point baseline (August 20 2025). During this period, internal surface disturbance developed on the glacier's middle and upper parts, and an internal surge front became marked at approximately 1.9 km distance from the reference terminus position. However, no downstream frontal propagation into the Dara River valley was detected.

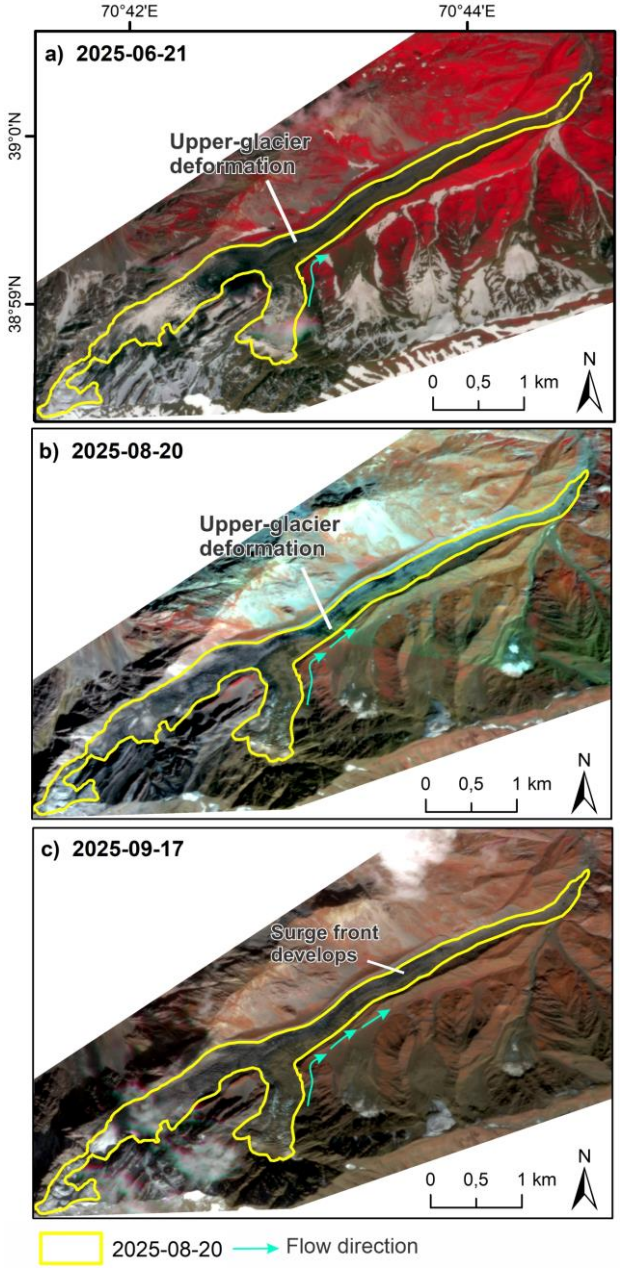

Figure 5: Progressive upper-glacier deformation and surge-front development at Dehdal Glacier prior to detachment, based on PlanetScope imagery (3 m resolution): (a) June 21, 2025, (b) August 20, 2025, and (c) September 17, 2025.

https://doi.org/10.5194/egusphere-2026-1923
Preprint. Discussion started: 22 April 2026

Between 17 and 21 September 2025, the glacier experienced detachment of its stagnant, debris-covered terminal sector. The detached ice was transported approximately 3.9 km down-valley relative to the 0-point, leaving a valley-blocking ice deposit near Safedob village (Fig. 6a). Because no satellite acquisitions were available within this interval, this displacement represents a minimum estimate of a sudden frontal jump rather than a resolved continuous velocity. This event marks the onset of the first detachment phase of surge propagation.

Following this initial detachment, the down-valley ice deposit remained quasi-stable until late October. During this period, the active glacier mass from the upper glacier rapidly re-advanced approximately 1.5 km down-valley, approaching the 0-point baseline. A second frontal detachment likely occurred around October 25 2025, affecting the lower glacier tongue. The detached ice flowed onto and over the previously deposited ice, advancing another ~0.8 km. Because clouds obscured the middle and upper glacier, the first cloud-free satellite image documenting this configuration was acquired on October 30 2025 and used for figure illustration and velocity analysis. The cumulative downstream displacement reached approximately 4.7 km by November 9 2025 (Figs. 8 and 9).

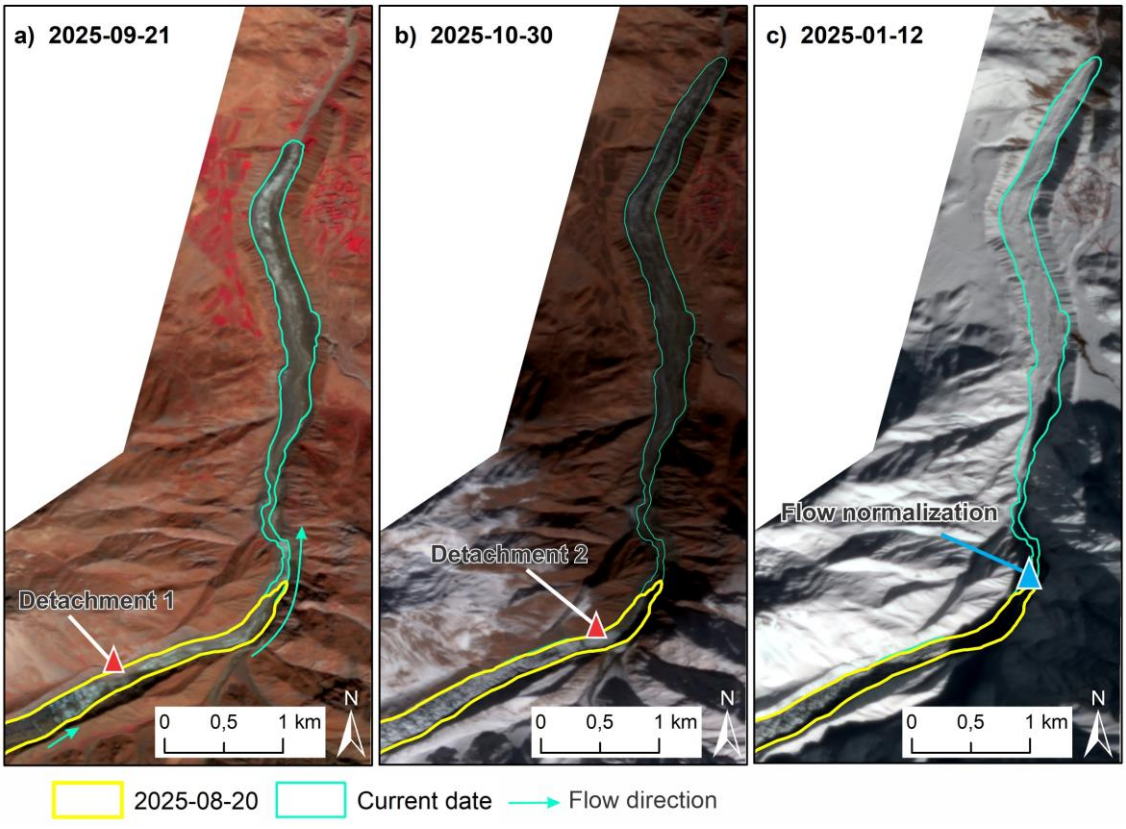

Figure 6: Detachment sequence and post-surge stabilization of Dehdal Glacier during the 2025–2026 surge derived from PlanetScope imagery (3 m resolution): (a) first detachment on September 21, 2025, involving separation of the stagnant debris-covered tongue; (b) second detachment on October 25, 2025, and visible on October 30, 2025, associated with renewed down-valley advance of the active tongue; (c) post-surge flow normalization observed on January 12, 2026. Yellow outlines show the glacier extent on August 20, 2025 (reference), and cyan outlines indicate glacier margins at each observation date. Arrows indicate ice-flow direction.

https://doi.org/10.5194/egusphere-2026-1923
Preprint. Discussion started: 22 April 2026

Unlike the first event, this second detachment was documented by residents and reported in Tajik media sources. Subsequently, the active glacier tongue accelerated and reoccupied the previously ice-free portion of the valley. UAV imagery acquired on December 2, 2025, reveals a clear mechanical separation between the dynamically connected main glacier tongue (primary tongue) and downstream detached ice masses (secondary tongue) (Figs. 10 and 11g–h). The active terminus reached and surpassed the 0-point baseline in early November 2025 and continued to advance thereafter. By January 12, 2026, the terminus had stabilized approximately 0.25 km down-valley from the reference position (Fig. 9). The three phases (internal surge, post-detachment 1, and post-detachment 2) exhibited distinct ice flow patterns and warrant further study to contrast the velocity, stress, and strain patterns controlling these instabilities.

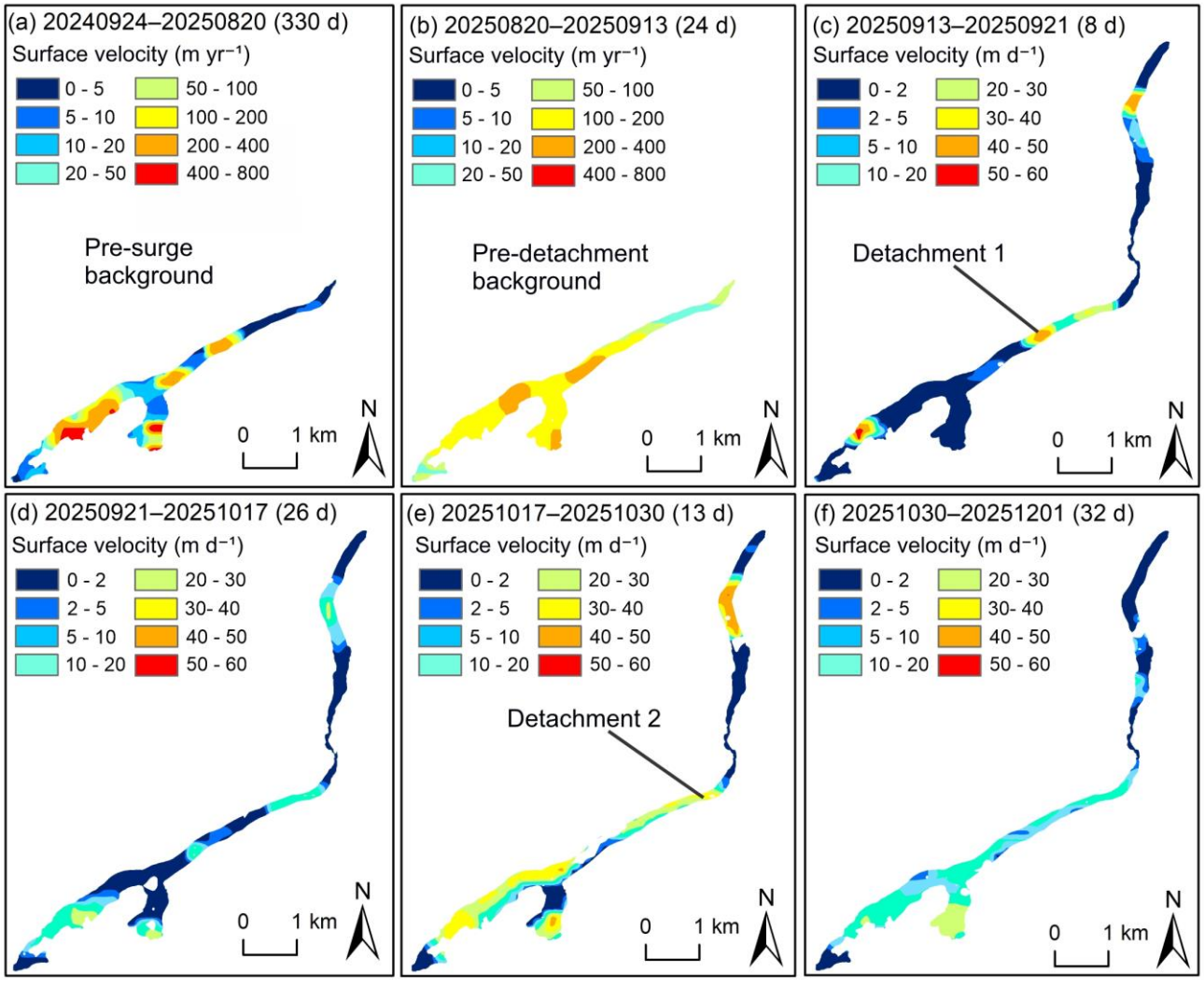

Figure 7: Surface velocity evolution during the 2025 Dehdal Glacier surge. (a) Interannual and background velocity (m yr⁻¹), (b) Pre-detachment background velocity (m yr⁻¹), and (c–f) Short-term velocities (m d⁻¹) during September–December 2025.

https://doi.org/10.5194/egusphere-2026-1923
Preprint. Discussion started: 22 April 2026

The pre-surge background velocity field (Fig. 7a), calculated for the period September 24, 2024–August 20, 2025, indicates generally low flow speeds across most of the glacier tongue, with velocities mostly below 200 m yr^{-1}. Localized zones of slightly elevated velocities occur near the confluence of tributary branches and along the lower trunk near locations A and B (Fig. 7a), suggesting areas of potential stress concentration prior to surge initiation. A clear transition from quiescent conditions to rapid glacier acceleration occurred after August 20 2025. During the first observation interval (August 20–September 13 2025; Fig. 7b), the glacier remained largely stagnant, with velocities mostly below 5 m d^{-1} across the main trunk. The subsequent short interval (13–21 September 2025; Fig. 6a) reveals the onset of rapid acceleration in the lower trunk and tributary confluence zone, where localized velocity maxima reached 40–50 m d^{-1}, coinciding with Detachment 1. The surge propagated further upstream during the period September 21–October 17, 2025 (Fig. 7d). Elevated velocities expanded along the central trunk of the glacier, while the tributary confluence region remained highly active. The following interval (17–30 October 2025; Fig. 7e) marks the peak stage of the surge, characterized by widespread acceleration across much of the glacier tongue and coinciding with Detachment 2. Maximum surface velocities reached ~56 m d^{-1} in the upper trunk and at the post-detachment terminus, indicating intense basal motion and strong longitudinal stress transfer along the glacier flowline. During the final observation period (October 30–December 1 2025; Fig. 7f), glacier motion began to decelerate. Although elevated velocities persisted in several sections of the lower trunk, overall speeds decreased substantially from the surge peak, suggesting that the glacier was transitioning back toward quiescent flow conditions. In addition, the flow patterns vary more smoothly along glacier length, suggesting that differential stress and strain regimes had largely equilibrated.

During the approximately four-month surge episode (September 2025–January 2026), Dehdal Glacier underwent rapid dynamic reorganization characterized by large frontal displacements and exceptionally high short-term flow velocities. The combined frontal displacement associated with the two detachment events exceeded ~4.7 km relative to the August 20, 2025, reference position. Peak surface velocities reached ~56 m d^{-1} during the late October surge maximum, representing more than two orders of magnitude acceleration relative to pre-surge background flow. The surge, therefore, involved both rapid basal motion and large-scale mechanical redistribution of ice within the glacier tongue, resulting in temporary occupation of previously ice-free downstream valley terrain.

4.3 Upper-glacier localization and branch-scale structural evolution

Multi-temporal satellite imagery and UAV orthomosaics acquired between 2019 and 2023 reveal pronounced structural weakening in the upper glacier before the 2025-2026 surge (Figs. 3 and S1–S2). The glacier splits into two main branches exhibiting strongly asymmetric pre-surge behaviour. The right branch displays progressive surface disruption, crevasse widening, debris displacement, and development of an incipient detachment zone between 2019 and 2023 (Fig. 8a-c), indicating increasing mechanical decoupling in the accumulation transport transition zone. In contrast, the left branch remained comparatively stable and largely passive. By November 2025, the right branch exhibited widespread post-surge deformation (Fig. 8d), confirming that surge initiation was localized at the tributary-branch scale and subsequently propagated down-glacier through segmented activation of the tongue.

https://doi.org/10.5194/egusphere-2026-1923
Preprint. Discussion started: 22 April 2026

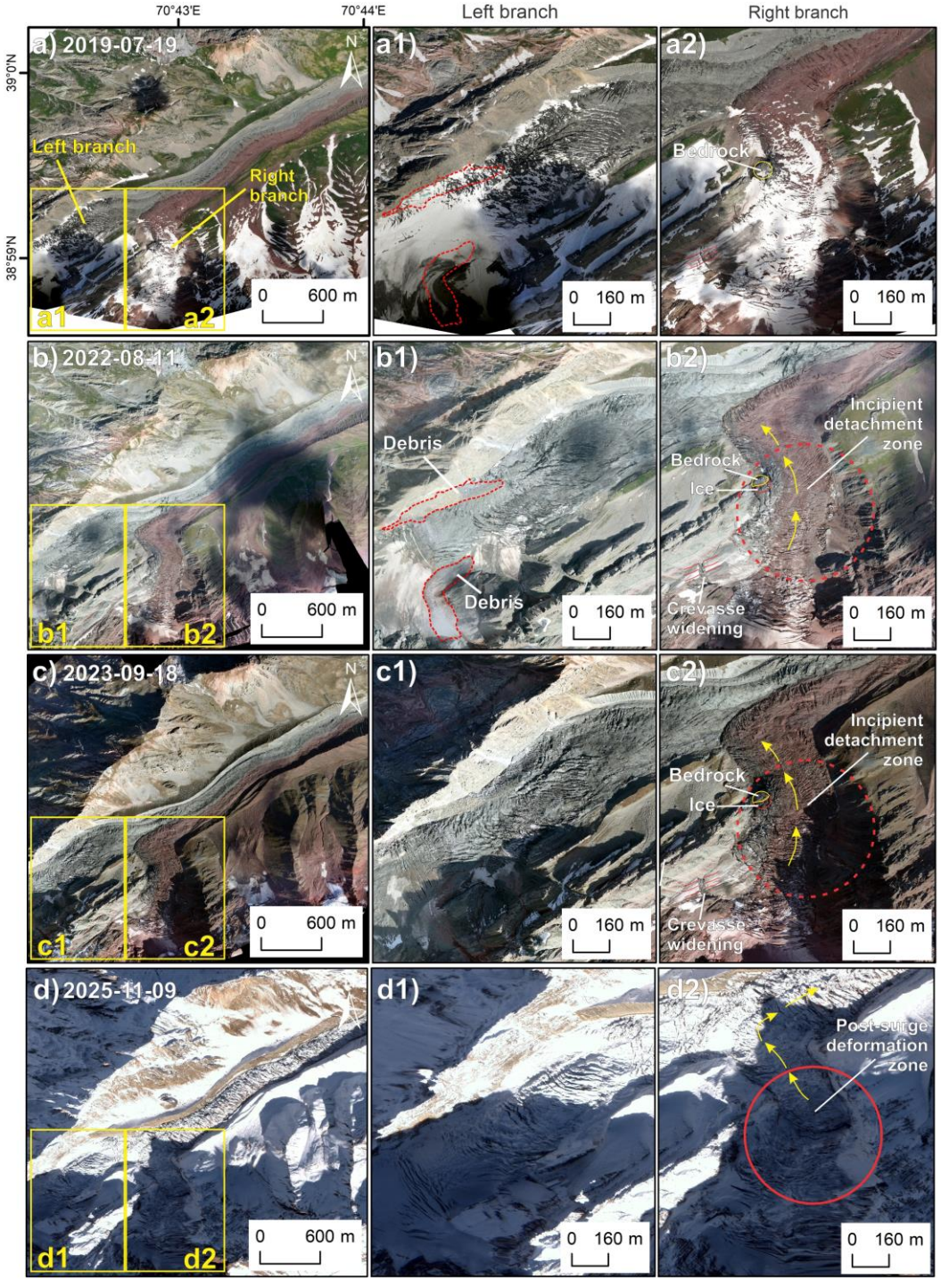

Figure 8: Structural evolution of the upper Dehdal Glacier between 2019 and 2025. (a–d) Satellite images acquired on July 19, 2019, August 11, 2022, September 18, 2023, and November 9, 2025. Panels (a1–d1) show the left branch of the upper glacier, and panels (a2–d2) show the right branch. Close-up views illustrate changes in surface texture, debris cover, crevasse patterns, and exposed bedrock. Yellow arrows indicate surface displacement features visible in the imagery.

https://doi.org/10.5194/egusphere-2026-1923
Preprint. Discussion started: 22 April 2026

4.4 Downstream valley occupation and geomorphic impact

Pre-surge imagery from 2019–2023 shows that the lower Dara River valley was ice-free prior to the 2025-2026 surge (Fig. 9b–f). By November 9, 2025, glacier ice and detached ice masses occupied the valley floor below Safedob village along a downstream reach exceeding ~4 km measured from the August 20, 2025, reference terminus (0-point) along the central flowline (Fig. 9b-c). The pre-surge glacier area on August 20, 2025, was 1.77 km². Following the first detachment on September 21 2025, a detached ice mass occupied approximately 0.21 km² of the downstream valley floor. Following the second detachment inferred around October 25, 2025, the total area of detached ice deposits increased to approximately 0.26 km². The resulting glacier configuration is first clearly visible in the cloud-free PlanetScope image acquired on October 30, 2025, indicating additional ice emplacement farther downstream. By January 12, 2026, the system had largely stabilized (Fig. 10). The primary glacier tongue covered approximately 1.83 km², while a detached ice mass (~0.26 km²) persisted farther downstream on the valley floor, separated from the main glacier by an active river channel. Based on the mean thickness derived from the cross-sectional profiles, the total deposited ice volume is estimated at approximately 4–5 × 10^6 m³. The combined mapped ice-covered area of the main glacier and detached ice bodies therefore reached approximately 2.09 km².

The newly emplaced ice substantially modified valley-floor morphology and channel geometry, indicating that the surge resulted not only in internal glacier reorganisation but also in significant reoccupation of downstream terrain that had remained ice-free for several decades prior to the event. UAV observations independently confirm post-surge occupation of the lower Dara valley by both the primary glacier tongue and detached ice masses (Fig. 11g–h).

https://doi.org/10.5194/egusphere-2026-1923
Preprint. Discussion started: 22 April 2026

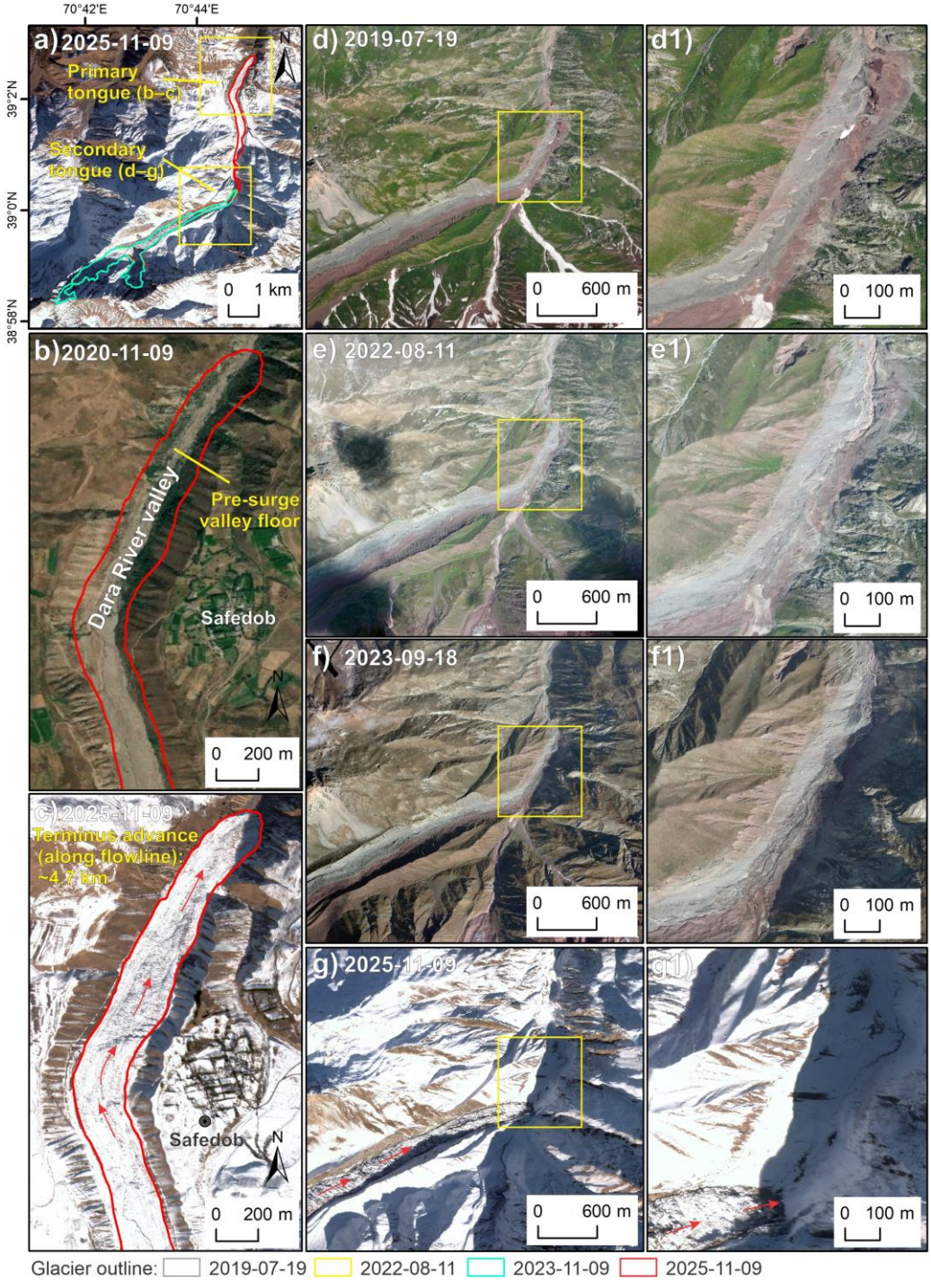

Figure 9: Downstream evolution of Dehdal Glacier before and after the 2025-2026 surge. (a) Overview of the glacier on November 9 2025, showing the spatial extent of glacier ice within the Dara River valley. (b) Pre-surge glacier extent on November 9 2020. (c) Post-surge terminus position on November 9 2025. (d–f) Downstream reach in 2019, 2022, and 2023, illustrating pre-surge surface conditions. (g) Downstream reach on November 9 2025. (d1–g1) Enlarged views of panels (d–g).

https://doi.org/10.5194/egusphere-2026-1923
Preprint. Discussion started: 22 April 2026

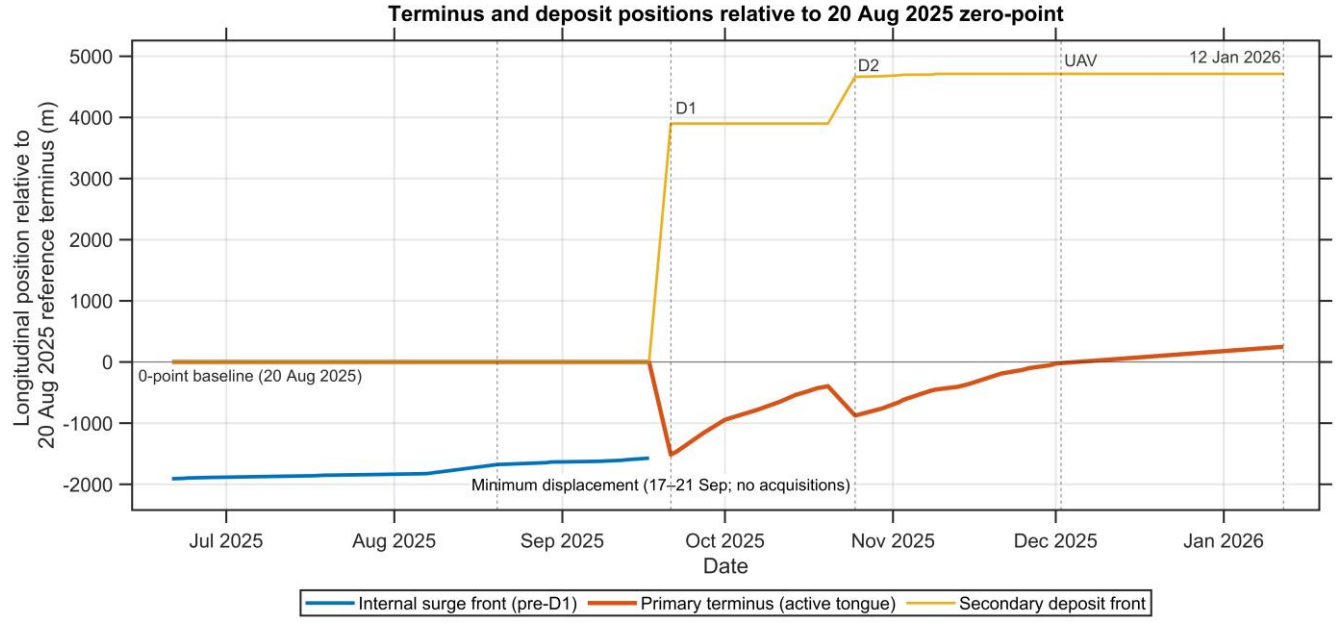

Figure 10: Flowline-projected longitudinal positions of the internal surge front, primary terminus (active tongue), and secondary deposit front of Dehdal Glacier relative to the August 20 2025, reference terminus (0-point). Positive values indicate down-valley displacement, whereas negative values denote up-glacier positions relative to the reference baseline.

https://doi.org/10.5194/egusphere-2026-1923
Preprint. Discussion started: 22 April 2026

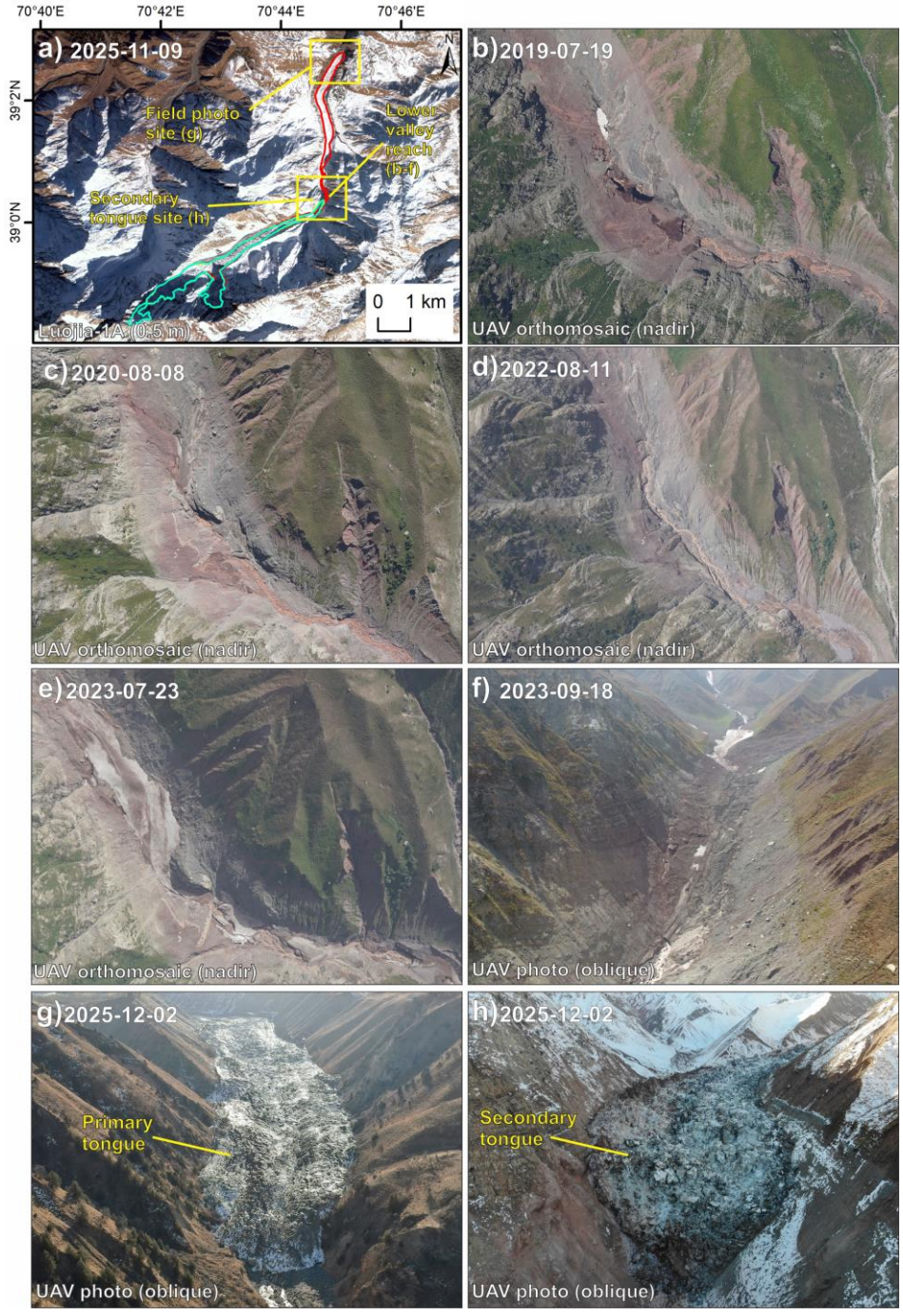

Figure 11: UAV field validation of post-surge valley occupation by Dehdal Glacier. (a) Luojia-1A image (0.5 m; November 9 2025) showing the spatial context of the lower Dara valley and locations of UAV survey sites (b–h). (b–e) UAV orthomosaics (nadir view) acquired in 2019, 2020, 2022, and 2023 demonstrate that the valley floor was ice-free before the 2025-2026 surge. (f) Oblique UAV view illustrating pre-surge valley morphology. (g–h) Oblique UAV photographs acquired on December 2 2025, documenting the physical occupation of the valley by both the primary and secondary surge tongues following the surge.

https://doi.org/10.5194/egusphere-2026-1923
Preprint. Discussion started: 22 April 2026

4.5 Seismicity and climate as supporting context

Regional earthquake records indicate persistent moderate seismic activity within a 60 km radius of Dehdal Glacier during 2019–2025 (Fig. 12a). Earthquake magnitudes during this period generally ranged between Mw 4.0 and 5.0, with the largest event reaching Mw 5.8 on April 13 2025 (Fig. 12b). No clear clustering of seismic events is observed immediately prior to the onset of rapid glacier acceleration in mid-2025. However, background tectonic activity remained continuous throughout the monitoring period. These observations indicate that the glacier is situated within an actively deforming tectonic environment, but do not demonstrate a temporally coincident seismic trigger.

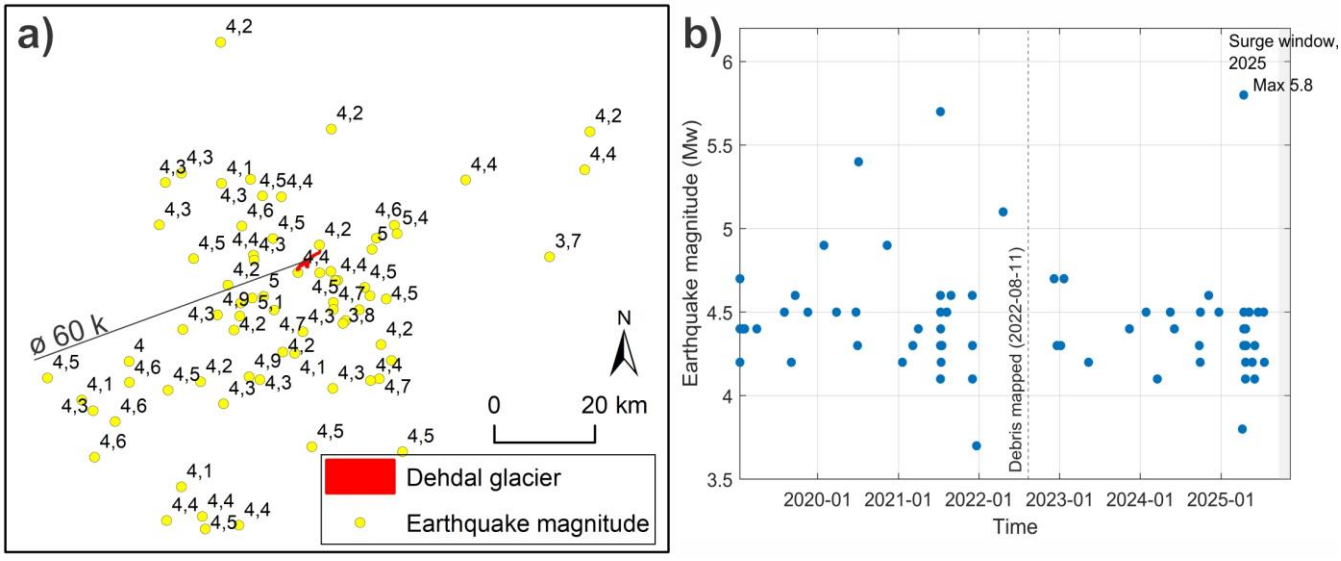

Figure 12: Regional seismicity surrounding Dehdal Glacier (2019–2025). (a) Spatial distribution of earthquakes (Mw ≥ 3.5) within 60 km of the glacier; (b) Temporal distribution of earthquake magnitudes relative to the 2025 surge window.

Monthly ERA5-Land data for 2016–2025 indicate a weak positive temperature tendency of approximately +0.14 °C yr^{-1} based on linear regression of annual mean temperatures (Fig. 13a), although the trend is not statistically significant (R^2 = 0.003; p = 0.57). Seasonal warming is most pronounced during late spring and summer months (Fig. 13c), with mean monthly anomalies relative to the 1981–2010 baseline reaching +1.11 °C (Fig. 14b). The largest positive temperature anomalies occur during May–September, corresponding to the ablation season.

Precipitation over 2016–2025 exhibits a weak negative linear trend (-1.55 mm yr^{-1}; R^2 = 0.017; p = 0.159; Fig. 13d), which is also statistically insignificant. Comparison with the 1981–2010 baseline indicates reduced precipitation during the warm season (May–September), with mean monthly anomalies of −26.4 mm and the strongest deficits occurring in mid-summer (Fig. 14d). No sustained increase in precipitation is observed during the decade preceding the surge. A recent study based on measurements at the Surkhob (Kyzylsu) Glacier, 62km to the east of Dehdal and at a similar altitude, also highlighted reduced precipitation as a major factor contributing to reduced glacier mass balances during the past decade (Jouberton et al., 2025).

https://doi.org/10.5194/egusphere-2026-1923
Preprint. Discussion started: 22 April 2026

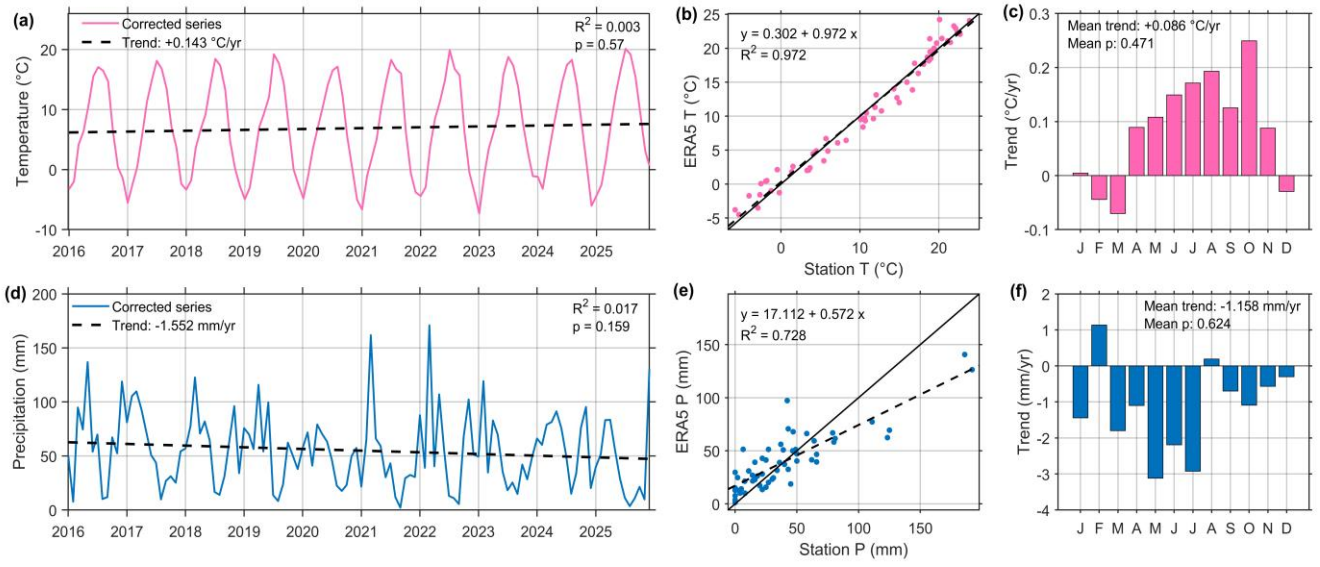

Figure 13: Climate variability and ERA5-Land validation for the Dehdal Glacier region (2016–2025). (a) Annual mean air temperature with linear trend. (b) Regression between the monthly station and ERA5-Land temperature. (c) Linear temperature trends for individual calendar months. (d) Annual total precipitation with linear trend. (e) Regression between the monthly station and ERA5-Land precipitation. (f) Linear precipitation trends for individual calendar months.

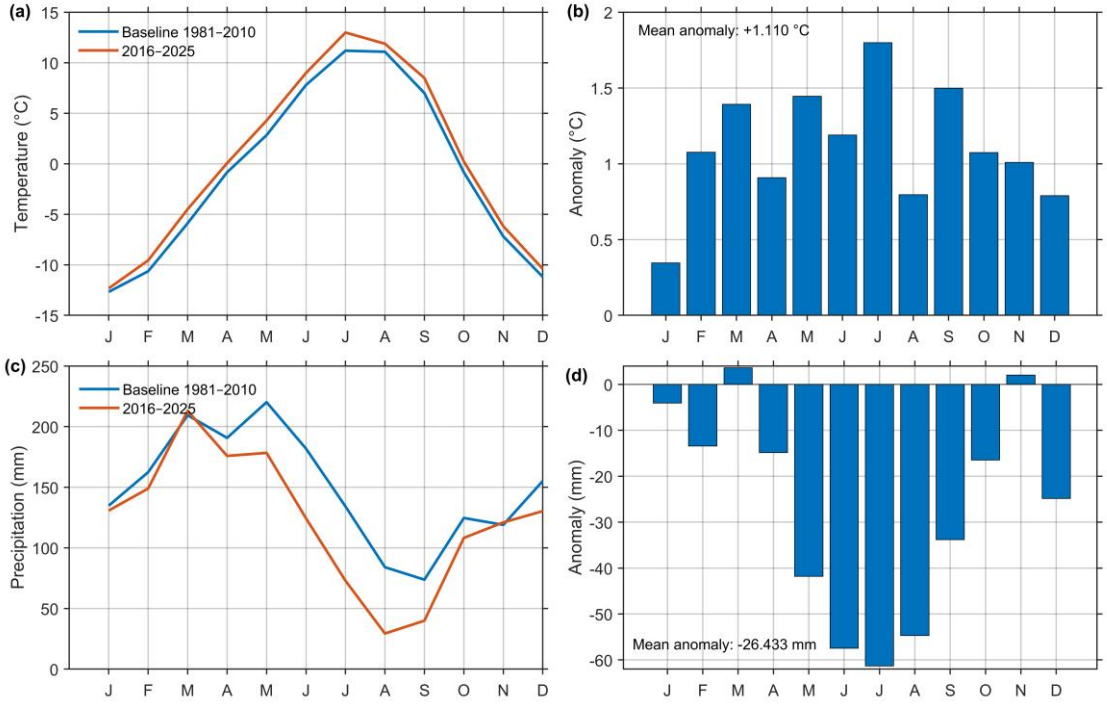

Figure 14: Comparison of ERA5-Land monthly air temperature and total precipitation between the baseline (1981–2010) and 2016–2025 at the Dehdal Glacier grid cell. (a) Mean monthly temperature. (b) Temperature anomalies (2016–2025 minus 1981–2010). (c) Mean monthly precipitation totals. (d) Precipitation anomalies, with the strongest reductions during May–September.

https://doi.org/10.5194/egusphere-2026-1923
Preprint. Discussion started: 22 April 2026

ERA5-Land temperature shows strong agreement with available Tojikobod station data (2020-2025) (R^2 = 0.972; Fig. 13b), while precipitation agreement is moderate (R^2 = 0.728; Fig. 13e), reflecting local variability and elevation differences between the station (1590 m asl) and glacier grid cell (2620 m asl). Collectively, these climatic and seismic data provide a regional background context for the 2025-2026 surge. The recent decade is characterised by warmer-than-baseline conditions and reduced precipitation, particularly during the ablation season. However, neither the monthly climatic trends nor the temporal distribution of regional seismic events demonstrates a clear temporal triggering relationship with the surge-collapse sequence.

5 Discussion

5.1 Segmented surge pulses and branch-scale initiation

The 2025–2026 surge of Dehdal Glacier represents an unusual case linking classical surge behaviour with low-angle detachment of the glacier tongue. Typically, surge-type glaciers are characterised by rapid acceleration followed by sustained frontal advance over periods of months to years (Meier and Post, 1969; Benn et al., 2019). In contrast, the 2025 event at Dehdal Glacier progressed through an internally generated surge pulse, complicated by two low-angle detachments of the glacier tongue. After separation from the main glacier, the displaced ice mass behaved as a dynamically independent ice-debris body rather than as a continuously flowing glacier terminus.

This behaviour shares characteristics with recently documented glacier instability and detachment events in high mountain environments (Faillettaz et al., 2015; Gilbert et al., 2018; Kääb et al., 2021). These studies show that rapid basal decoupling and mechanical weakening can trigger sudden glacier break-off or collapse, producing large ice-debris masses that travel several kilometres downstream. The Dehdal event, therefore, illustrates how surge-driven acceleration may transition into mechanical detachment of a debris-covered glacier tongue. Unlike many surge-type glaciers in the Karakoram and Pamir, where surge acceleration involves large sections of the glacier trunk (Bhambri et al., 2017; Safarov et al., 2024a), the Dehdal event instead shows spatially localized surge initiation within a single tributary branch. Multi-year velocity observations reveal that the right tributary experienced progressive acceleration beginning several years prior to the 2025 event, whereas the left tributary remained comparatively stable.

The pre-surge velocity fields and longitudinal profiles (Fig. 4) indicate that acceleration was concentrated within the right tributary between approximately 4 and 5 km upstream from the terminus. This spatial pattern suggests that surge initiation developed within a confined tributary source region before activating the lower glacier trunk. Similar tributary-scale surge initiation has been documented in several surge-type glaciers in High Mountain Asia, where localized stress accumulation or hydrological reorganization can trigger surge activation within specific glacier sectors (Copland et al., 2011; Sevestre and Benn, 2015; Lv et al., 2019; Li et al., 2023).

Structural observations from multi-temporal satellite imagery and UAV data further support this interpretation. Progressive crevasse widening, debris displacement, and the development of an incipient detachment zone in the right tributary between

https://doi.org/10.5194/egusphere-2026-1923
Preprint. Discussion started: 22 April 2026

2019 and 2023 indicate mechanical destabilization prior to the surge, consistent with observations linking crevasse formation to glacier acceleration (Nanni et al., 2025). These structural changes closely match the velocity anomalies observed along the right tributary of the glacier and suggest that surge initiation was preceded by localized weakening of the glacier structure within the tributary confluence zone.

The resulting surge behaviour therefore reflects a combination of localized dynamic initiation and subsequent surge propagation through the glacier trunk, culminating in detachment of the terminal tongue. Similar glacier detachments and rock-ice avalanche processes have been documented elsewhere in the Peter I Range of Tajikistan (Leinss et al., 2021), indicating that valley confinement, glacier geometry, and local geological conditions may promote mechanically unstable glacier behaviour in this region.

5.2 Topographic and mechanical controls on the detachment of the glacier tongue

The detachment of the Dehdal Glacier tongue during the 2025–2026 surge likely resulted from the interaction between surge-driven acceleration and local topographic and mechanical conditions within the lower glacier valley. Glacier detachments typically occur where rapid glacier acceleration coincides with weak basal coupling, strong longitudinal stress gradients, and gravitational forcing along steep valley slopes (Faillettaz et al., 2015; Kääb et al., 2021).

One important factor is the confined valley geometry of the lower Dehdal Glacier. The glacier tongue occupies a narrow valley that strongly constrains lateral spreading and promotes efficient transmission of longitudinal stress during periods of rapid flow. Such geometric confinement can amplify compressional and extensional stress fields within the glacier tongue, increasing the likelihood of mechanical rupture during surge acceleration. Similar behaviour has been observed in confined valley glaciers where surge propagation produces strong stress concentration near the glacier terminus (Sevestre and Benn, 2015; Lovell et al., 2026).

The debris-covered character of the lower glacier tongue may have contributed to mechanical instability. Thick supraglacial debris modifies the surface energy balance and can locally suppress ablation, allowing ice to accumulate and thicken during the quiescent phase (Benn et al., 2012; Gilbert et al., 2018). During surge acceleration, this stored mass can increase longitudinal stress gradients within the glacier tongue (Sevestre and Benn, 2015a; Faillettaz et al., 2015). Debris-covered glacier tongues are known to develop complex internal stress regimes and structural weaknesses that can favour mechanical failure under rapid dynamic forcing (Benn et al., 2012; Gilbert et al., 2018; Kääb et al., 2021).

The rapid acceleration observed in September–October 2025 suggests that basal hydrological conditions played an important role. Increased meltwater production during recent warm summers, particularly during 2025, may have enhanced basal lubrication beneath the glacier tongue. Elevated basal water pressure can reduce effective normal stress at the glacier bed and promote rapid basal sliding, a process widely invoked in surge-type glacier dynamics (Clarke, 1987; Sevestre and Benn, 2015; Benn et al., 2019). If basal water pressure approaches ice overburden pressure, basal coupling may weaken sufficiently to permit detachment of the glacier tongue. Moreover, clay-rich subglacial sediments reported in parts of the regional geology may further reduce basal shear strength and facilitate mechanical decoupling under high water pressure conditions, a

https://doi.org/10.5194/egusphere-2026-1923
Preprint. Discussion started: 22 April 2026

mechanism proposed for several recent glacier detachment events (Jacquemart et al., 2020; Kääb et al., 2021; Leinss et al., 2021).

The slope of the lower glacier tongue may have further facilitated rapid down-valley displacement once detachment occurred. Elevation profiles indicate that the lowermost ~1 km of the glacier tongue has a mean slope of approximately 13°, with local slopes reaching ~28°. Slopes within this range have been associated with several documented glacier detachment events in high mountain environments, where gravitational driving stresses become sufficiently large to promote rapid sliding or collapse (Kääb et al., 2021).

Taken together, these observations suggest that the 2025-2026 Dehdal Glacier event resulted from a combination of surge-induced acceleration, basal hydrological weakening, debris-covered tongue dynamics, and strong valley-scale geometric confinement. Once mechanical decoupling occurred, gravitational driving stresses likely facilitated rapid down-valley displacement of the detached ice mass, producing the large displacement observed during the two detachment events.

5.3 Geomorphic impacts and hazard implications of surge-detachment events

The 2025–2026 surge of Dehdal Glacier demonstrates that even relatively small debris-covered mountain glaciers can produce substantial geomorphic disturbance when surge acceleration culminates in glacier tongue detachment. The two detachment events transported large volumes of glacier ice several kilometres downstream, rapidly occupying previously ice-free sections of the Dara River valley. Such rapid redistribution of ice and debris can substantially modify valley-floor morphology, alter river channels, and enhance sediment delivery to downstream fluvial systems (Gilbert et al., 2018; Muhammad et al., 2021; Meng et al., 2023; Lovell et al., 2026).

Prior to the surge, satellite and UAV imagery indicate that the lower Dara River valley remained largely ice-free between 2019 and 2023. Following the detachment events, however, detached ice masses occupied more than 4 km of the valley floor downstream of the pre-surge glacier terminus. This rapid emplacement of ice represents a major geomorphic perturbation that temporarily altered the valley-floor landscape. Similar valley-floor reoccupation has been documented following large glacier detachments and ice-debris avalanches in other high mountain regions, where rapid ice displacement reshapes valley morphology and modifies river networks (Gilbert et al., 2018; Kääb et al., 2021).

Rapid glacier advance or detachment-driven displacement can temporarily obstruct river channels, increase sediment flux, or trigger secondary processes such as debris flows and debris floods in mountain catchments (Haeberli et al., 2017; Baggio et al., 2024; Murodov et al., 2024). In confined mountain valleys, these processes can propagate downstream, affecting settlements or transportation routes along river corridors. Although no catastrophic flooding occurred during the Dehdal event of 2025, the presence of detached ice masses and altered river channels indicates that surge-detachment events may represent a previously under-recognized cryospheric hazard in the Pamir Mountains. The 1974 Dehdal event was reported to be accompanied by numerous outburst floods during the active phase. The estimated detached ice volume of ~4–5 × 10^6 m^3 is smaller than the largest glacier detachment documented in the Petra Pervogo Range (8.8 × 10^6 m^3; Leinss et al., 2021) but

https://doi.org/10.5194/egusphere-2026-1923
Preprint. Discussion started: 22 April 2026

remains within the same order of magnitude as previously reported glacier detachments in the region. This suggests that the Dehdal Glacier event represents another example of large-scale glacier instability typical of the Pamir Mountains.

The Dehdal event also highlights the importance of high-frequency satellite monitoring for detecting and analysing rapid glacier instabilities. The daily PlanetScope observations used in this study allowed the full evolution of the surge and detachment sequence to be reconstructed at high temporal resolution. Many historical surge events in High Mountain Asia have been reconstructed from annual or multi-annual satellite imagery, which limits the ability to resolve short-lived dynamic processes such as detachment events or rapid surge pulses (Goerlich et al., 2020). High-frequency observations, therefore, provide critical new insights into the short-term kinematics of glacier instabilities.

More broadly, the observations presented here suggest that surge-type behaviour in small debris-covered glaciers may produce geomorphic impacts that extend well beyond the glacier terminus. In steep, confined mountain valleys such as those of the Pamir region, surge-driven detachments may allow glacier ice to rapidly advance into downstream terrain that has remained ice-free for decades. These processes highlight the need for improved monitoring of dynamically unstable glaciers and for greater integration of glacier surge behaviour into regional assessments of cryospheric hazards in High Mountain Asia. These observations indicate that small debris-covered glaciers in steep mountain environments should be included in regional monitoring frameworks, as surge-detachment cascades may occur rapidly and produce significant geomorphic disturbance even in relatively small glacier systems.

5.4 Implications for surge dynamics in small debris-covered glaciers

The observations presented here indicate that surge behaviour in small debris-covered glaciers may evolve along dynamic pathways that differ from those described by the classical surge model. In the case of Dehdal Glacier, the surge was preceded by multi-year dynamic reorganisation within a single tributary branch, followed by rapid surge propagation and ultimately mechanical detachment of the glacier tongue. These observations demonstrate that surge acceleration may, under certain geometric and mechanical conditions, culminate in structural failure of the glacier tongue rather than sustained frontal advance. In classical surge-type glaciers, accelerated ice typically remains dynamically connected to the glacier trunk and produces sustained frontal advance (Meier and Post, 1969; Benn et al., 2019), whereas at Dehdal Glacier, surge acceleration culminated in the mechanical separation of the glacier tongue.

The Dehdal event, therefore, illustrates a dynamic continuum between surge-type glacier behaviour and low-angle glacier detachment processes. While classical surge theory assumes that accelerated ice remains dynamically connected to the glacier trunk, the observations presented here show that surge-driven stress transfer can instead lead to mechanical separation of the terminal glacier tongue. After detachment, the displaced ice mass moved rapidly down-valley under the force of gravity. Similar detachment mechanisms have been documented in several recent glacier collapse events in High Mountain Asia (Gilbert et al., 2018; Kääb et al., 2021), suggesting that such behaviour may represent an under-recognised end-member of surge dynamics in steep mountain environments.

https://doi.org/10.5194/egusphere-2026-1923
Preprint. Discussion started: 22 April 2026

These findings highlight the importance of glacier geometry and valley confinement in controlling surge expression (Sevestre and Benn, 2015a; Lovell et al., 2026). In narrow valleys with relatively steep lower tongues, surge-induced acceleration may generate sufficiently large longitudinal stress gradients to promote structural rupture within the glacier tongue. Under such conditions, surge propagation may transition into detachment-driven displacement rather than continuous glacier advance. This mechanism may be particularly relevant for small debris-covered glaciers, where strong topographic control and heterogeneous ice thickness can produce localized mechanical instabilities (Benn et al., 2012).

The daily PlanetScope observations used in this study provide rare high-temporal-resolution insight into the short-term evolution of surge-driven glacier instabilities. High-frequency satellite observations therefore offer new opportunities to investigate the short-term processes governing glacier instabilities and surge behaviour in remote mountain regions.

These results indicate that surge-type glaciers in steep mountain environments may exhibit a broader spectrum of dynamic behaviour than previously recognised. In particular, surge acceleration may transition into glacier tongue detachment, producing rapid downstream displacement of glacier ice. Such surge-detachment cascades may represent an under-recognised dynamic pathway in small debris-covered glaciers that occupy steep, confined valleys. Similar geometric and mechanical conditions occur widely across High Mountain Asia (Leinss et al., 2021; Kääb et al., 2021; Zou et al., 2023; Guo et al., 2023), suggesting that comparable surge-driven detachment processes may be more common than previously documented. Recognizing this surge-detachment transition is therefore important for improving understanding of glacier instability processes and for assessing cryospheric hazards associated with dynamically unstable mountain glaciers.

5.5 Research priorities for surge-detachment events

Several unresolved questions emerging from the Dehdal Glacier event define priorities for future investigation of surge–detachment cascades in steep mountain glaciers:

Climate influence and shortened surge recurrence: The ~9–10-year interval between the 2015–2016 and 2025–2026 events is considerably shorter than the multi-decadal cycles previously documented at this site. Although ERA5-Land data indicate warmer-than-baseline conditions during the preceding decade, the mechanisms linking climate forcing to shortened surge recurrence remain unclear. Future work should examine whether increased meltwater generation and longer ablation seasons could accelerate basal hydrological reorganization and trigger earlier surge activation before full reservoir regeneration. The enthalpy model of surging (Benn et al, 2019) may provide a useful framework for this assessment, but must explain the transition point between efficient and inefficient mass evaluation at Dehdal Glacier.

Role of basal materials and debris composition: The mechanical behaviour of the glacier tongue may depend strongly on the properties of basal sediments. Fine-grained or clay-rich subglacial materials can reduce basal shear strength and promote rapid decoupling under elevated water pressures. Field sampling of debris and valley-floor deposits, combined with grain-size and geotechnical analyses, could help determine whether weak basal sediments contributed to the low-angle detachments observed at Dehdal Glacier.

https://doi.org/10.5194/egusphere-2026-1923
Preprint. Discussion started: 22 April 2026

Fracture mechanics and stress evolution preceding detachment: The two detachment events differed in geometry and displacement patterns, suggesting differences in stress balance and failure processes. Future analyses should examine time-evolving strain-rate fields, driving stress variations, and fracture propagation within the glacier tongue. Integrating high-frequency velocity fields with simplified stress modeling would help clarify how surge acceleration transitions into mechanical rupture.

Controls on surge versus surge-detachment behaviour: Historical observations indicate that Dehdal Glacier has experienced surges with varying frontal responses, ranging from conventional advance to detachment-driven displacement. Understanding why some surges produce only advance while others culminate in glacier tongue collapse requires comparison of glacier geometry, valley confinement, debris thickness, and basal hydrology across different surge cycles. Systematic comparison of the 1974, 2015–2016, and 2025–2026 events may help identify thresholds controlling the transition from classical surge behaviour to surge-detachment cascades.

Taken together, the observations from Dehdal Glacier indicate that surge-type behaviour in small debris-covered glaciers may evolve through a dynamic cascade involving localized surge initiation, rapid surge propagation, and mechanical detachment of the glacier tongue. This sequence highlights a previously under-recognized pathway linking classical surge dynamics with glacier collapse processes in steep mountain environments. Such surge-detachment transitions may therefore represent an important but poorly documented component of glacier instability in High Mountain Asia.

6 Conclusions

This study documents a surge-driven glacier detachment event at Dehdal Glacier in the northwestern Pamirs using daily PlanetScope imagery, UAV surveys, and multi-year velocity analysis. The results provide new insights into the dynamics of surge-type glaciers in steep mountain environments.

I. The surge exhibited a stepwise evolution characterized by two low-angle detachment events. Surge initiation occurred within the right tributary of the glacier several years prior to the event and subsequently propagated downstream through the glacier trunk before culminating in mechanical detachment of the debris-covered tongue.
II. Detachment of the glacier tongue resulted from the interaction between surge acceleration and local geometric and mechanical controls. Valley confinement, debris-covered tongue dynamics, basal hydrological weakening, and relatively steep valley slopes likely promoted mechanical decoupling and rapid down-valley displacement of glacier ice.
III. The surge-detachment cascade produced substantial geomorphic disturbance in the lower Dara River valley. Detached ice masses occupied more than 4 km of previously ice-free valley floor, demonstrating that even small debris-covered glaciers can rapidly modify downstream landscapes during surge events.

https://doi.org/10.5194/egusphere-2026-1923
Preprint. Discussion started: 22 April 2026

IV. These observations highlight a bridge between classical surge behaviour and glacier detachment processes. Surge acceleration in steep, confined valleys may, under certain conditions, culminate in structural failure of the glacier tongue rather than sustained frontal advance.

V. High-frequency satellite observations are critical for resolving short-term glacier instabilities. The daily PlanetScope imagery used in this study enabled reconstruction of surge initiation, propagation, and detachment processes at unprecedented temporal resolution, providing new opportunities to investigate rapidly evolving glacier hazards in High Mountain Asia.

Taken together, these findings demonstrate that small debris-covered glaciers can generate complex surge-detachment cascades with significant geomorphic and hazard implications. This highlights the importance of systematic high frequency monitoring of dynamically unstable glaciers to improve understanding of glacier instability processes and associated cryospheric hazards across High Mountain Asia.

Author contributions

MS contributed to conceptualization, methodology, data curation, formal analysis, software, validation, visualization, and writing (original draft and review and editing). JL contributed to conceptualization, methodology, investigation, data curation, writing (original draft and review and editing), funding acquisition, supervision, and project administration. EM contributed to methodology, formal analysis, validation, and writing (review and editing). MG contributed to methodology and investigation. RL contributed to methodology, validation, and data curation. AF, KN, and FV contributed to investigation and data curation. MM contributed to investigation, data curation, and software. HN contributed to investigation and data curation. AH contributed to investigation and software. All authors read and approved the final manuscript.

Declaration of Competing Interest

The authors declare that they have no known competing financial interests or personal relationships that could have appeared to influence the work reported in this paper

Data availability

The datasets supporting this study are publicly available at Zenodo: https://doi.org/10.5281/zenodo.19052838

Acknowledgements

https://doi.org/10.5194/egusphere-2026-1923
Preprint. Discussion started: 22 April 2026

We thank Planet Labs PBC for providing PlanetScope satellite imagery through the Planet Education and Research Program, and Wuhan University for providing the high-resolution Luojia-1A satellite image used in this study. Sentinel satellite data provided by the Copernicus Programme and the AW3D30 digital elevation model produced by the Japan Aerospace Exploration Agency (JAXA) were also used in this study. We are grateful to local collaborators and field assistants for their assistance during fieldwork in the Dara River valley.

Funding

This research was supported by the National Natural Sciences Foundation of China (U2003201) and Natural Science Foundation of Xinjiang Uygur Autonomous Region (2023D01E18).

References

Baggio, T., Martini, M., Bettella, F., and D'Agostino, V.: Debris flow and debris flood hazard assessment in mountain catchments, Catena, 245, 108338, https://doi.org/10.1016/j.catena.2024.108338, 2024.

Benn, D. I., Bolch, T., Hands, K., Gulley, J., Luckman, A., Nicholson, L. I., Quincey, D., Thompson, S., Toumi, R., and Wiseman, S.: Response of debris-covered glaciers in the Mount Everest region to recent warming and implications for outburst flood hazards, Earth-Sci. Rev., 114, 156–174, https://doi.org/10.1016/j.earscirev.2012.03.008, 2012.

Benn, D. I., Fowler, A. C., Hewitt, I., and Sevestre, H.: A general theory of glacier surges, J. Glaciol., 65, 701–716, https://doi.org/10.1017/jog.2019.62, 2019.

Bhambri, R., Hewitt, K., Kawishwar, P., and Pratap, B.: Surge-type and surge-modified glaciers in the Karakoram, Sci. Rep., 7, 15391, https://doi.org/10.1038/s41598-017-15473-8, 2017.

Clapuyt, F., Vanacker, V., Schlunegger, F., and Van Oost, K.: Unravelling Earth flow dynamics with 3-D time series derived from UAV-SfM models, Earth Surf. Dyn., 5, 791–806, https://doi.org/10.5194/esurf-5-791-2017, 2017.

Clarke, G. K. C.: Fast glacier flow: ice streams, surging, and tidewater glaciers, J. Geophys. Res., 92, 8835–8841, https://doi.org/10.1029/JB092iB09p08835, 1987.

Copland, L., Sylvestre, T., Bishop, M. P., Shroder, J. F., Seong, Y. B., Owen, L. A., and Kamp, U.: Expanded and recently increased glacier surging in the Karakoram, Arct. Antarct. Alp. Res., 43, 503–516, https://doi.org/10.1657/1938-4246-43.4.503, 2011.

Dehecq, A., Gourmelen, N., and Trouve, E.: Deriving large-scale glacier velocities from a complete satellite archive: application to the Pamir–Karakoram–Himalaya, Remote Sens. Environ., 162, 55–66, https://doi.org/10.1016/j.rse.2015.01.031, 2015.

Desinov, S. L.: Recent glacier movements in the western part of the Peter the Great Ridge (Pamir), Earth's Cryosphere, 25, 47–56, https://doi.org/10.15372/KZ20210405, 2021 (in Russian).

https://doi.org/10.5194/egusphere-2026-1923
Preprint. Discussion started: 22 April 2026

Faillettaz, J., Funk, M., and Vincent, C.: Avalanching glacier instabilities: a review of processes and early warning perspectives, Rev. Geophys., 53, 203–224, https://doi.org/10.1002/2014RG000466, 2015.

Farinotti, D., Immerzeel, W. W., de Kok, R. J., Quincey, D. J., and Dehecq, A.: Manifestations and mechanisms of the Karakoram glacier anomaly, Nat. Geosci., 13, 8–16, https://doi.org/10.1038/s41561-019-0513-5, 2020.

Feroz, A., Liang, S., Li, G., Li, X., Rahman, Z. U., and Yang, B.: Debris-covered glaciers mapping based on machine learning and multi-source satellite images over Eastern Pamir, Big Earth Data, 9, 265–297, https://doi.org/10.1080/20964471.2025.2463726, 2025.

Fowler, A. C., Murray, T., and Ng, F. S. L.: Thermally controlled glacier surging, J. Glaciol., 47, 527–538, https://doi.org/10.3189/172756501781831792, 2001.

Gilbert, A., Leinss, S., Kargel, J., Kääb, A., Gascoin, S., Leonard, G., Berthier, E., Karki, A., and Yao, T.: Mechanisms leading to the 2016 giant twin glacier collapses in the Aru Range, Tibet, Cryosphere, 12, 2883–2900, https://doi.org/10.5194/tc-12-2883-2018, 2018.

Goerlich, F., Bolch, T., and Paul, F.: More dynamic than expected: an updated survey of surging glaciers in the Pamir, Earth Syst. Sci. Data, 12, 3161–3176, https://doi.org/10.5194/essd-12-3161-2020, 2020.

Guillet, G., King, O., Lv, M., Ghuffar, S., Benn, D., Quincey, D., and Bolch, T.: A regionally resolved inventory of High Mountain Asia surge-type glaciers derived from a multi-factor remote sensing approach, Cryosphere, 16, 603–623, https://doi.org/10.5194/tc-16-603-2022, 2022.

Guo, L., Li, J., Dehecq, A., Li, Z., Li, X., and Zhu, J.: A new inventory of High Mountain Asia surging glaciers derived from multiple elevation datasets since the 1970s, Earth Syst. Sci. Data, 15, 2841–2861, https://doi.org/10.5194/essd-15-2841-2023, 2023.

Haeberli, W., Schaub, Y., and Huggel, C.: Increasing risks related to landslides from degrading permafrost into new lakes in deglaciating mountain ranges, Geomorphology, 293, 405–417, 2017.

Heid, T. and Kääb, A.: Evaluation of existing image matching methods for deriving glacier surface displacements globally from optical satellite imagery, Remote Sens. Environ., 118, 339–355, https://doi.org/10.1016/j.rse.2011.11.024, 2012.

Hersbach, H., Bell, B., Berrisford, P., et al.: The ERA5 global reanalysis, Q. J. R. Meteorol. Soc., 146, 1999–2049, https://doi.org/10.1002/qj.3803, 2020.

Immerzeel, W. W., Kraaijenbrink, P. D., Shea, J. M., Shrestha, A. B., Pellicciotti, F., Bierkens, M. F., and de Jong, S. M.: High-resolution monitoring of Himalayan glacier dynamics using unmanned aerial vehicles, Remote Sens. Environ., 150, 93–103, https://doi.org/10.1016/j.rse.2014.04.025, 2014.

Jacquemart, M., Loso, M., Leopold, M., Welty, E., Berthier, E., Hansen, J. S., Sykes, J., and Tiampo, K.: What drives large-scale glacier detachments? Insights from Flat Creek glacier, St. Elias Mountains, Alaska, Geology, 48, 703–707, https://doi.org/10.1130/G47211.1, 2020.

Jiskoot, H.: Glacier surging, in: Encyclopaedia of Snow, Ice and Glaciers, edited by: Singh, V. P., Singh, P., and Haritashya, U. K., Springer, Heidelberg, 415–428, 2011.

https://doi.org/10.5194/egusphere-2026-1923
Preprint. Discussion started: 22 April 2026

Jouberton, A., Shaw, T. E., Miles, E., Kneib, M., Fugger, S., Buri, P., McCarthy, M., Kayumov, A., Navruzshoev, H., Halimov, A., Kabutov, K., Homidov, F., and Pellicciotti, F.: Snowfall decrease in recent years undermines glacier health and meltwater resources in the Northwestern Pamirs, Commun. Earth Environ., 6, 691, https://doi.org/10.1038/s43247-025-02611-8, 2025.

Kääb, A.: Remote sensing of mountain glaciers and permafrost creep, Phys. Geogr. Ser., 48, University of Zürich, 2005.

Kääb, A., Jacquemart, M., Gilbert, A., Leinss, S., Girod, L., Huggel, C., Falaschi, D., Ugalde, F., Petrakov, D., Chernomorets, S., Dokukin, M., Paul, F., Gascoin, S., Berthier, E., and Kargel, J. S.: Sudden large-volume detachments of low-angle mountain glaciers – more frequent than thought?, Cryosphere, 15, 1751–1785, https://doi.org/10.5194/tc-15-1751-2021, 2021.

Kamb, B., Raymond, C. F., Harrison, W. D., Engelhardt, H., Echelmeyer, K. A., Humphrey, N., Brugman, M. M., and Pfeffer, T.: Glacier surge mechanism: 1982–1983 surge of Variegated Glacier, Alaska, Science, 227, 469–479, https://doi.org/10.1126/science.227.4686.469, 1985.

Kotlyakov, V. M., Desinov, L. V., Desinov, S. L., and Rudakov, V. A.: Surges of the Pamir glaciers in the first 20 years of the 21st century, Dokl. Earth Sci., 495, 854–857, https://doi.org/10.1134/S1028334X20110082, 2020.

Lamsters, K., Ješkins, J., Sobota, I., Karušs, J., and Džeriņš, P.: Surface characteristics, elevation change, and velocity of high-Arctic valley glacier from repeated high-resolution UAV photogrammetry, Remote Sens., 14, 1029, https://doi.org/10.3390/rs14041029, 2022.

Leinss, S., Bernardini, E., Jacquemart, M., and Dokukin, M.: Glacier detachments and rock-ice avalanches in the Petra Pervogo range, Tajikistan (1973–2019), Nat. Hazards Earth Syst. Sci., 21, 1409–1429, https://doi.org/10.5194/nhess-21-1409-2021, 2021.

Li, G., Lv, M., Quincey, D. J., Taylor, L. S., Li, X., Yan, S., Sun, Y., and Guo, H.: Characterizing the surge behaviour and associated ice-dammed lake evolution of the Kyagar Glacier in the Karakoram, Cryosphere, 17, 2891–2907, https://doi.org/10.5194/tc-17-2891-2023, 2023.

Lipskiy, V. I.: Mountainous Bukhara: results of three-year journeys to Central Asia in 1896, 1897 and 1899, Part 2: Gissar, Peter the Great Ridge, Alay, St. Petersburg, 1902 (in Russian).

Lovell, H., Benn, D. I., Jiskoot, H., et al.: Glacier surging and surge-related hazards in a changing climate, Nat. Rev. Earth Environ., https://doi.org/10.1038/s43017-025-00757-9, 2026.

Lv, M., Guo, H., Lu, X., Liu, G., Yan, S., Ruan, Z., Ding, Y., and Quincey, D. J.: Characterizing the behaviour of surge- and non-surge-type glaciers in the Kingata Mountains, eastern Pamir, from 1999 to 2016, Cryosphere, 13, 219–236, https://doi.org/10.5194/tc-13-219-2019, 2019.

Meier, M. F. and Post, A.: What are glacier surges?, Can. J. Earth Sci., 6, 807–817, https://doi.org/10.1139/e69-081, 1969.

Meng, Z., Lyu, L., Xu, M., Yu, G., Ma, C., Wang, Z., and Stoffel, M.: Effects of frequent debris flows on barrier lake formation, sedimentation and vegetation disturbance, Palongzangbo River, Tibetan Plateau, Catena, 220, 106697, https://doi.org/10.1016/j.catena.2022.106697, 2023.

https://doi.org/10.5194/egusphere-2026-1923
Preprint. Discussion started: 22 April 2026

Mishra, A., Nainwal, H. C., Bolch, T., Shah, S. S., and Shankar, R.: Glacier inventory and glacier changes (1994–2020) in the Upper Alaknanda Basin, Central Himalaya, J. Glaciol., 69, 591–606, https://doi.org/10.1017/jog.2022.87, 2023.

Muhammad, S., Li, J., Steiner, J. F., Shrestha, F., Shah, G. M., Berthier, E., and Tian, L.: A holistic view of Shisper Glacier surge and outburst floods: from physical processes to downstream impacts, Geomat. Nat. Hazards Risk, 12, 2755–2775, https://doi.org/10.1080/19475705.2021.1975833, 2021.

Murodov, M., Li, L., Safarov, M., Lv, M., Murodov, A., Gulakhmadov, A., Khusrav, K., and Qiu, Y.: A comprehensive examination of the Medvezhiy Glacier's surges in West Pamir (1968–2023), Remote Sens., 16, 1730, https://doi.org/10.3390/rs16101730, 2024.

Nanni, U., Bouchayer, C., Akesson, H., et al.: Observed positive feedback between surface ablation and crevasse formation drives glacier acceleration and potential surge, Nat. Commun., 16, 11227, , 2025.

Osipova, G., Tchetinnikov, A., and Rudak, M.: Catalogue of surging glaciers of Pamir, Mater. Glyatsiol. Issled., 85, 3–136, 1998 (in Russian).

Paul, F., Bolch, T., Briggs, K., Kääb, A., McMillan, M., McNabb, R., Nagler, T., Nuth, C., Rastner, P., Strozzi, T., and Wuite, J.: Error sources and guidelines for quality assessment of glacier area, elevation change, and velocity products derived from satellite data in the Glaciers_cci project, Remote Sens. Environ., 203, 256–275, https://doi.org/10.1016/j.rse.2017.08.038, 2017.

Planet Labs PBC: PlanetScope imagery product documentation, available at: https://docs.planet.com/data/imagery/planetscope/ (last access: 20 January 2026), 2026.

Quincey, D. J., Braun, M., Glasser, N. F., Bishop, M. P., Hewitt, K., and Luckman, A.: Karakoram glacier surge dynamics, Geophys. Res. Lett., 38, L18504, https://doi.org/10.1029/2011GL049004, 2011.

Ravier, É., Lelandais, T., Vérité, J., and Bourgeois, O.: Variations in hydraulic efficiency of the subglacial drainage landsystem control surging and streaming regimes of outlet glaciers, J. Glaciol., 69, 860–878, https://doi.org/10.1017/jog.2022.107, 2023.

Raymond, C. F.: How do glaciers surge? A review, J. Geophys. Res., 92, 9121–9134, https://doi.org/10.1029/JB092iB09p09121, 1987.

RGI Consortium: Randolph Glacier Inventory – a dataset of global glacier outlines, version 6, NSIDC, Boulder, CO, USA, https://doi.org/10.7265/4m1f-gd79, 2017.

RGI Consortium: Randolph Glacier Inventory – a dataset of global glacier outlines, version 7, NSIDC, Boulder, CO, USA, https://doi.org/10.5067/F6JMOVY5NAVZ, 2023.

Rototayev, K. P.: Advance of Lednik Didal' in the Pamir, Mater. Glyatsiol. Issled., 24, 188, 1974 (in Russian).

Rounce, D. R., Hock, R., and Shean, D. E.: Glacier mass change in High Mountain Asia through 2100 using the open-source Python glacier evolution model (PyGEM), Front. Earth Sci., 7, 331, https://doi.org/10.3389/feart.2019.00331, 2020.

Safarov, M., Kang, S., Murodov, M., et al.: Quantifying glacier surging and associated lake dynamics in Amu Darya River basin using UAV and remote sensing data, J. Mt. Sci., 21, 2967–2985, https://doi.org/10.1007/s11629-023-8538-z, 2024a.

https://doi.org/10.5194/egusphere-2026-1923
Preprint. Discussion started: 22 April 2026

Safarov, M., Kang, S., Fazylov, A., et al.: Estimating glacier dynamics and supraglacial lakes together with associated regional hazards using high-resolution datasets in the Pamir, J. Mt. Sci., 21, 3767–3788, https://doi.org/10.1007/s11629-024-8936-x, 2024b.

Safarov, M. S. and Fazylov, A. R.: Remote sensing and monitoring of mudflow-prone areas in the mountainous territories of Tajikistan, Promexpo, Dushanbe, 2023 (in Russian).

Scambos, T. A., Dutkiewicz, M. J., Wilson, J. C., and Bindschadler, R. A.: Application of image cross-correlation to the measurement of glacier velocity using satellite image data, Remote Sens. Environ., 42, 177–186, https://doi.org/10.1016/0034-4257(92)90101-O, 1992.

Sevestre, H. and Benn, D. I.: Climatic and geometric controls on the global distribution of surge-type glaciers: implications for a unifying model of surging, J. Glaciol., 61, 646–662, https://doi.org/10.3189/2015JoG14J136, 2015a.

Sevestre, H., Benn, D. I., and Hulton, N. R. J.: Thermal structure of Svalbard glaciers and implications for thermal switch models of glacier surging, J. Geophys. Res. Earth Surf., 120, 2220–2236, 2015b.

Tarca, G., Hoelzle, M., and Guglielmin, M.: Using PlanetScope images to investigate the evolution of small glaciers in the Alps, Remote Sens. Appl. Soc. Environ., 32, 101013, https://doi.org/10.1016/j.rsase.2023.101013, 2023.

Wang, Z., Jiang, Z., Wu, K., Liu, S., Zhang, Y., Wang, X., Zhang, Z., and Wei, J.: Characteristics of glaciers surging in the western Pamirs, Remote Sens., 15, 1319, https://doi.org/10.3390/rs15051319, 2023.

Wheaton, J. M., Brasington, J., Darby, S. E., and Sear, D. A.: Accounting for uncertainty in DEMs from repeat topographic surveys: improved sediment budgets, Earth Surf. Process. Landf., 35, 136–156, https://doi.org/10.1002/esp.1886, 2010.

Xue, Y., Jing, Z., Kang, S., He, X., and Li, C.: Combining UAV and Landsat data to assess glacier changes on the central Tibetan Plateau, J. Glaciol., 67, 862–874, https://doi.org/10.1017/jog.2021.37, 2021.

Zhang, T., Wang, W., Shen, Z., Zhan, N., Wang, Z., and An, B.: Understanding the 2004 glacier detachment in the Amney Machen Mountains, northeastern Tibetan Plateau, via multi-phase modeling, Landslides, 20, 315–330, https://doi.org/10.1007/s10346-022-01989-2, 2023.

Zou, C., Jansen, J. D., Carling, P. A., Dou, X., Wei, Z., and Fan, X.: Triggers for multiple glacier detachments from a low-angle valley glacier in the Amney Machen Range, eastern Tibetan Plateau, Geomorphology, 440, 108867, https://doi.org/10.1016/j.geomorph.2023.108867, 2023.